DEVELOPMENT OF A

BY

SURNAME, FIRST NAME OTHER NAME

MATRIC NO

A B. Sc Project Presented for the

Award of Bachelor of Science Degree in Computer Science,

Department of Computer Science,

Faculty of Science,

National Open University of Nigeria, Abuja , Nigeria.

JUNE, 2016

CERTIFICATION

This report with the title:

Development of a

Submitted by

SURNAME, FIRST NAME OTHER NAME

(MATRIC NO)

Has partially satisfied the regulation governing the award of the degree of

Bachelor of Science (B. Sc) Degree in Computer Science

National Open University of Nigeria, Abuja, Nigeria.

.....	.....
Prof. S.O. Olabiyisi	**Date**
Supervisor	
.....	.....
Dr.	**Date**
Head of Department	

DEDICATION

This thesis is dedicated to the Almighty God, my source of wisdom and the giver of life.

ACKNOWLEDGEMENT

I give thanks to the Almighty God for giving me the strength and courage to get to this stage of my life. Also, for His continuous protection and provision in my life. May His name be continually praised and exalted.

My heartfelt appreciation goes to my supervisor Prof. S. O. Olabiyisi

My sincere appreciation also goes to the Head of Department, Computer Science ,,,,,,,,,,,,,,,,,,,,,,,,,,,,,,,,,,,, for her support towards the progress of this research. Also, I appreciate the contribution of the entire staff of the Department of Computer Science and for their encouragement and supports. God bless you all.

I also really appreciate the special love, provision and support of my parents,

ABSTRACT

Reconstruction techniques are meant for reconstructing low resolution images to high resolution images required in various fields such as medicine. Most existing image reconstruction techniques constitute high image distortions which consequently increase their reconstruction error. Hence, this research developed a Discrete Algebraic Back Projection Reconstruction Technique (DABPRT) to reconstruct low resolution images.

A total of fifty (50) Low Resolution (LR) images were obtained using vivicam digital camera of 5 Mega Pixel (MP). The DABPRT was developed by combining Discrete Algebraic Reconstruction Technique (DART) and Iterative Back Projection (IBP) using composition operation. The acquired images were reconstructed to high resolution images by minimizing the associated blur, noise and warp from the images using DART while the resulting reconstruction error was minimized using IBP component of the developed DABPRT. The DABPRT was implemented in Matrix Laboratory 8.0 (R2012a) and evaluated by comparing it with the existing DART and IBP using Peak Signal to Noise Ratio (PSNR), Structural Similarity (SSIM) and Mean Square Error (MSE). The results obtained were tested statistically using Analysis of Variance (ANOVA) to determine the significance difference between the developed DABPRT and the existing DART and IBP at α = 0.05.

The result of the evaluation showed that DART produced an average PSNR, SSIM and MSE of 71.7025dB, 1.0 and 0.00479, respectively while IBP produced an average PSNR, SSIM and MSE of 82.425dB, 1.0 and 0.00077, respectively. The developed DABPRT produced an average PSNR, SSIM and MSE OF 85.435Db, 1.0 and 0.000385, respectively which was statistically significant using ANOVA test.

This research developed a reconstruction technique that serves as an improvement over DART and IBP in terms of PSNR and MSE. It could be adopted by medical practitioners to reconstruct images acquired from low resolution image capturing devices.

TABLE OF CONTENTS

CHAPTER FIVE

CONCLUSION AND RECOMMENDATION

LIST OF FIGURES

LIST OF TABLES

CHAPTER ONE

INTRODUCTION

1.1 Background to the Study

Image processing is a method used to convert an image into digital form and performing some operations on it, in order to get an enhanced image or to extract some useful information from it (Kavita, *et al*, 2013). It uses signal dispensation in which input is image, like video frame or photograph and output may be image or characteristics associated with that image.

Analog and digital image processing are the two forms of image processing. Analog techniques of image processing can be used for the hard copies like printouts and photographs. Digital processing technique helps in the manipulation of digital images by using computers (Kavita *et al.*, 2013). Digital image processing is used to extract pictorial details along with useful information from the given image of lower quality. High resolution (HR) can be described as when the pixel density within an image is high; therefore an HR image can offer more detailed information that may be critical in various applications. For example, HR medical images are very helpful for a doctor to make a correct diagnosis.

It may be easy to distinguish an object from similar ones using HR satellite images, the performance of pattern recognition in computer vision can be improved if an HR image is provided. Since the 1970s, charge-coupled device (CCD) and Complementary metal-oxide semiconductor (CMOS) image sensors have been widely used to capture digital images. Although, these sensors are suitable for most imaging applications, the current resolution level and consumer price has not satisfied the future demand (Farrell and Wandell, 2015).

In applications like satellite imaging, medical imaging, microscopy, security systems, archeology study. It is most desirable to have images with detailed information. In other words

higher resolution images are most preferred for their detailed information also, high resolution (HR) images provide better edge details, classification of regions along with a more detailed view of the human eye (Bengtsson, 2013).

Digital image processing enhances the features of interest and extracting useful information about the scene from the enhanced image (Ansari, 2013). High-resolution images and videos are important in many applications such as astronomy, military monitor, medical diagnosis among others, super resolution (SR) reconstruction has a great significance in obtaining images with more detailed information (Yixiong, *et al*, 2015).

Super-resolution image reconstruction is a technique of digital imaging which attempts to reconstruct LR images by fusing the partial information contained within a number of under sampled low-resolution (LR) images of that scene during the image reconstruction process (Anil and Vijay, 2014). Super-resolution image reconstruction includes up-sampling of under-sampled images thereby removing distortions such as noise and blur. In comparison to various image enhancement techniques, super-resolution image reconstruction technique does not only improve the quality of under-sampled, low-resolution images by increasing their spatial resolution but also attempts to filter out distortions such as noise (Anil and Vijay, 2014).

1.2 Statement of Problem

High resolution images are needed because they contain high pixel density. The requirement to view and analyze visual information of images with greater details increases in medical, satellite and security applications. The best image acquisition systems are expensive and existing image reconstruction techniques still have high reconstruction error. (Fasiu, 2004).

Discrete Algebraic Reconstruction Technique (DART) stems from discrete tomography (DT), which tackles the problem of recovering images from their projections, where the images

are assumed to consist of a small number (2 to 5) of gray values only (Zefreh, Aarle, Batenburg and Sijbers, 2013). If the set of gray levels is known or estimated in advance, this prior knowledge can be used by the DT reconstruction algorithm.

The Iterative Back Projection (IBP) based reconstruction is an inversion problem using the gradient descent method to find a solution. Since inverse problems are ill-posed problems, they need regularization or optimization of the solution (Wang and Yanfei, 2011). DART is less optimal but highly efficient (Zefreh *et al*. 2013), whereas IBP is more optimal in nature but less efficient. Combining the two techniques provided a more efficient and reliable technique with higher visual quality output. Therefore, in this research, a combined DART and IBP technique for super resolution reconstruction is developed.

1.3 Aim and Objectives

The aim of this research is to develop a discrete algebraic back projection reconstruction technique to reconstruct low resolution images.

The specific objectives of this research are to:

i. design a discrete algebraic back projection technique for the reconstruction of low resolution images;
ii. implement the designed technique proposed in (i);
iii. evaluate the performance of the proposed technique over IBP and DART using Peak Signal to Noise Ratio (PSNR), Structural Similarity(SSIM) and Mean Square Error (MSE) as metrics.

1.4 Significance of Study

The image sensors limit the spatial resolution of the image, while the image details (high-frequency bands) are also limited by the optics, due to lens blurs associated with sensor point

spread function (PSF), lens aberration effects, aperture diffractions and optical blurring due to motion (Agrawal, 2013). Constructing imaging chips and optical components to capture very high resolution images are expensive and not practical in most real applications, for example, widely used surveillance and cell phone built-in cameras (Merugu and Kamal, 2013). Besides the cost of high resolution image capturing devices, the resolution of a surveillance camera is limited in camera storage and hardware storage. Therefore, embarking on this research helped to realize low cost super resolution reconstruction technique that is both highly optimal and efficient.

1.5 Scope of Study

A number of super resolution reconstruction techniques exist in principle for low resolution image enhancement. However, in this research, Iterative Back Projection and Discrete Algebraic Reconstruction Techniques were only considered to reconstruct 50 low resolution images. Furthermore, Peak Signal to Noise Ratio (PSNR), Structural Similarity Index (SSIM) and Mean Square Error (MSE) are the performance evaluation metrics that were used.

CHAPTER TWO

LITERATURE REVIEW

2.1 Image Processing

Image processing is a method of converting an image into digital form and performing some operations on it, in order to get an enhanced image or to extract some useful information

from it. It is a type of signal dispensation in which the input is image, like video frame or photograph and output may be image or characteristics associated with that image (Amit and Avinash, 2013). The overall objective of the system is to reconstruct low resolution images into high resolution images.

Image processing usually refers to digital image processing, but analog image processing is also possible. Image processing has the following steps; Importing the image with optical scanner or by digital capturing device; Analyzing and manipulating the image which includes data compression and image enhancement and spotting patterns that are not visible to human eyes like satellite photographs; output is the last stage in which results can be altered image or report that is based on image analysis (Kavita *et al.,* 2013). Image processing is done for five various purposes, which are; visualization which is to observe the objects that are not visible, image sharpening and restoration which helps to create a better image, image retrieval, seeking for the image of interest, measurement of patterns and image recognition which is to distinguish the objects in an image.

2.1.1 Analog image processing

Analog image processing refers to the alteration of image through electrical means. The most common example is the television image (Muzamil, 2014). The television signal is a voltage level which varies in amplitude to represent brightness through the image. By electrically varying the signal, the displayed image appearance is altered. The brightness and contrast controls on a TV set serve to adjust the amplitude and reference of the video signal, resulting in the brightening, darkening and alteration of the brightness range of the displayed image (Rao, 2006).

Analog or visual technique of image processing can also be used for hardcopies like printouts and photographs. Image analysts use various fundamentals of interpretation while using these visual techniques. Image processing is not just confined to area that has to be studied but on

knowledge of analyst. Association is another important tool in image processing through visual techniques, so analysts apply a combination of personal knowledge and collateral data to image processing (Muzamil, 2014).

2.1.2 Digital image processing

Digital image processing generally refers to the processing of a two-dimensional picture by a digital computer (Ramesh, 2012). It refers to digital processing of any two-dimensional data. It is defined as the subjecting numerical representations of objects to a series of operations in order to obtain a desired result (Muzamil, 2014). It starts with one image and produces a modified version of the same image. It is therefore a process that takes an image into another. To get over flaws and to get originality of information, it has to undergo various phases of processing. The three general phases that all types of data undergo while using digital technique are Pre-processing, enhancement and display and information extraction (Rao, 2006). A digital image is an array of real numbers represented by a finite number of bits. The main advantages of digital image processing method are its versatility, repeatability and the preservation of original data precision. As raw data from imaging sensors from satellite platform contains deficiencies.

2.2 Image Processing Techniques

There are different image processing techniques, they are; Image representation; Image Preprocessing; Image enhancement; Image restoration; Image analysis; Image reconstruction and Image data compression.

2.2.1 Image representation

An image defined in the "real world" is considered to be a function of two real variables, for example, $f(x, y)$ where f is the amplitude (such as brightness) of the image at the real

coordinate position (x, y) (Kavita *et al.*, 2013). The effect of digitalization is shown in figure 2.1. The 2D continuous image $f(x, y)$is divided into N rows and M columns. The intersection of a row and column is called a pixel. The value assigned to the integer coordinates $[m, n]$where $\{m = 0,1,2,...,M-1\}$and $\{n = 0,1,2,...,N-1\}$is $f[m, n]$ (Kavita *et al.*, 2013). In most cases $f(x, y)$ is considered to be the physical signal that impinges on the face of a sensor. Typically an image file such as BMP, JPEG, TIFF, has some header and picture information. A header usually includes details like format identifier, resolution, number of bits/pixel and compression type.

2.2.2 Image preprocessing

Image preprocessing involves scaling. The purpose of the technique of magnification is to have a closer view by magnifying or zooming the interested part in the image (Jyoti and Bhubneshwar, 2015). By reduction, an unmanageable size of data can be brought to a manageable limit. For resampling an image, Nearest Neighborhood, Linear, or cubic convolution techniques are used.

2.2.2.1 Magnification: This is usually done to improve the scale of display or geometrical size for visual interpretation or sometimes to match the scale of one image to another. To

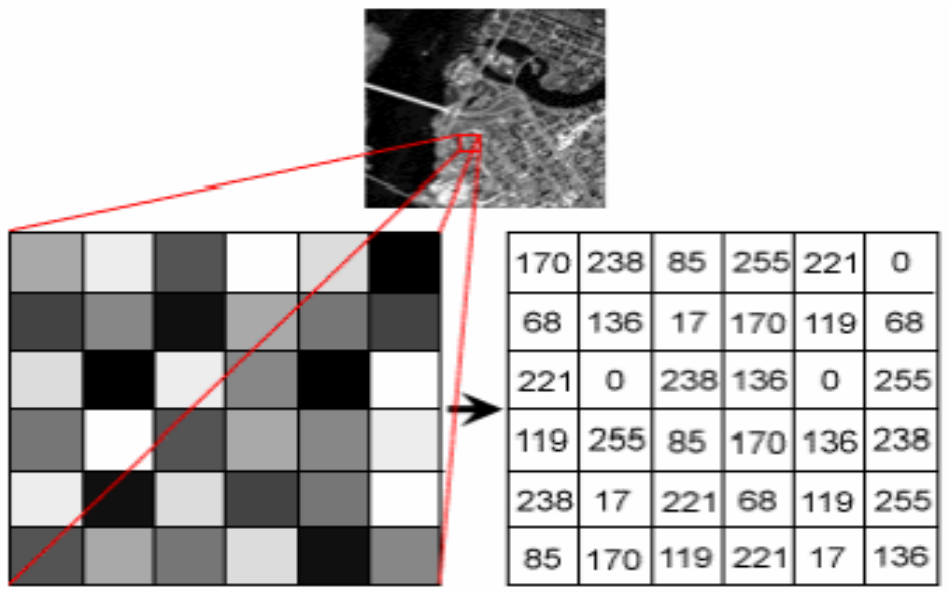

Figure 2.1: Effect of Digitalization (Rao, 2006).

magnify an image by a factor of 2, each pixel of the original image is replaced by a block of 2x2 pixels, all with the same brightness value as the original pixel.

2.2.2.2 Reduction: This is used to reduce a digital image to the original data, every m^{th} row and m^{th} column of the original imagery is selected and displayed. Another way of accomplishing this is by taking the average in 'm x m' block and displaying the average after proper rounding of the resultant value (Rao, 2006).

2.2.2.3 Rotation: Rotation is used in image mosaic, image registration etc. One of the techniques of rotation is 3-pass shear rotation, where rotation matrix can be decomposed into three separable matrices (Muzamil, 2014).

2.2.2.4 Mosaic: Mosaic is a process of combining two or more images to form a single large image without radiometric imbalance. Mosaic is required to get the synoptic view of the entire area, otherwise capture as small images (Muzamil, 2014).

2.2.3 Image enhancement

Sometimes image obtained from satellites and conventional and digital cameras lack in contrast and brightness because of the limitation of imaging sub systems and illumination conditions while capturing image (Jyoti and Bhubneshwar, 2015). Images may have different types of noise. In image enhancement, the goal is to accentuate certain image features for subsequent analysis or for image display (Ramesh, 2012). Examples include contrast and edge enhancement, pseudo-coloring, noise filtering, sharpening, and magnifying.

Image enhancement is relevant in feature extraction, image analysis and an image display. The enhancement process itself does not increase the inherent information content in the data. It simply emphasizes certain specified image characteristics. Enhancement algorithms are generally interactive and application-dependent. Some image enhancement techniques include contrast stretching, noise filtering and histogram modification.

2.2.3.1 Contrast stretching: some images (for example over water bodies, deserts, dense forest, snow, clouds and under hazy conditions over heterogeneous regions) are homogenous that is, they do not have much change in their levels. In terms of histogram representation, they are characterized as the occurrence of very narrow peaks (Ramesh, 2012). The homogeneity can also be due to the incorrect illumination of the scene. Ultimately, the images obtained are not easily interpretable due to poor human perceptibility. This is because there is only a narrow range of gray-levels in the image having provision for wider range of gray-levels. The contrast stretching methods are designed exclusively for frequently encountered situations (Rao, 2006).

2.2.3.2 Noise filtering: this is used to filter unnecessary information and distortion from an image. It is also used to remove various types of noises from the images (Muzamil, 2014). Mostly this feature is interactive. Various filters like low pass, high pass, mean, median etc., are available.

2.2.3.3 Histogram modification: Histogram has a lot of relevance in image enhancement. It reflects the characteristics of image. By modifying the histogram, image characteristics can be modified (Rao, 2006). One of such example is Histogram Equalization. Histogram equalization is a nonlinear stretch that redistributes pixel values so that there is approximately the same number of pixels with each value within a range (Rao, 2006). The result approximates a flat histogram. Therefore, contrast is increased at the peaks and lessened at the tails.

2.2.4 Image restoration

Image restoration refers to removal or minimization of degradations in an image. This includes de-blurring of images degraded by the limitations of a sensor or its environment, noise filtering, and correction of geometric distortion or non-linearity due to sensors (Ramesh, 2012). Image is restored to its original quality by inverting the physical degradation phenomenon such as defocus, linear motion, atmospheric degradation and additive noise.

2.2.5 Image analysis

Image analysis is concerned with making quantitative measurements from an image to produce a description of it (Ramesh, 2012). In the simplest form, this task could be reading a label on a grocery item, sorting different parts on an assembly line, or measuring the size and orientation of blood cells in a medical image. More advanced image analysis systems measure quantitative information and use it to make a sophisticated decision, such as controlling the arm of a robot to move an object after identifying it or navigating an aircraft with the aid of images acquired along its trajectory.

Image analysis techniques require extraction of certain features that help in the identification of the object (Rao, 2006). Segmentation techniques are used to isolate the desired object from the scene so that measurements can be made on it subsequently. Quantitative measurements of object features allow classification and description of the image. Image segmentation is the process that subdivides an image into its constituent parts or objects. The level to which this subdivision is carried out depends on the problem being solved, that is, the segmentation should stop when the objects of interest in an application have been isolated.

2.2.6 Image reconstruction from projections

Image reconstruction from projections is a special class of image restoration problems where a two (or higher) dimensional object is reconstructed from several one-dimensional projections (Ramesh, 2012). Each projection is obtained by projecting a parallel X-ray (or other penetrating radiation) beam through the object. Planar projections are thus obtained by viewing the object from many different angles. Reconstruction algorithms derive an image of a thin axial slice of the object, giving an inside view otherwise unobtainable without performing extensive surgery. Such techniques are important in medical imaging, astronomy, radar imaging, geological exploration, and nondestructive testing of assemblies.

2.2.7 Image data compression

Compression is a very essential tool for archiving image data, image data transfer on the network etc. (Rao, 2006). There are various techniques available for lossy and lossless compressions. One of most popular compression techniques, JPEG (Joint Photographic Experts Group) uses Discrete Cosine Transformation (DCT) based compression technique. Currently wavelet based compression techniques are used for higher compression ratios with minimal loss of data (Ramesh, 2012).

2.3 Super Resolution

Super resolution (SR) is a class of techniques that enhance the resolution of an imaging system (Gaidhani, 2012).The main aim of Super-Resolution (SR) is to generate a higher resolution image from lower resolution images. High resolution images offer a high pixel density and thereby more details about the original scene (Gaidhani, 2012). The need for high resolution is common in computer vision applications for better performance in pattern recognition and analysis of images. High resolution is of importance in medical imaging for diagnosis. Many applications require

zooming of a specific area of interest in the image wherein high resolution becomes essential, for example surveillance, forensic and satellite imaging applications.

However, high resolution images are not always readily available because they are expensive and also it may not always be feasible due to the inherent limitations of the sensor, optics manufacturing technology. These problems can be solved through the use of image processing algorithms, which are relatively inexpensive, giving rise to concept of super-resolution (Rao *et al*. 2013). It provides an advantage as it may cost less and the existing low resolution imaging systems can still be utilized.

Super-resolution (SR) are techniques that construct high-resolution (HR) images from several observed low-resolution (LR) images, thereby increasing the high frequency components and removing the degradations caused by the imaging process of the low resolution camera. The basic idea behind SR is to combine the non-redundant information contained in multiple low-resolution frames to generate a high-resolution image. A closely related technique with SR is the single image interpolation approach, which can be also used to increase the image size (Milanfar, 2010).

Super-resolution is based on the idea that a combination of low resolution (noisy) sequence of images of a scene can be used to generate a high resolution image or image sequence. Thus it attempts to reconstruct the original scene image with high resolution given a set of observed images at lower resolution. The general approach considers the low resolution images as resulting from resampling of a high resolution image. The goal is then to recover the high resolution image which when resampled based on the input images and the imaging model, will produce the low resolution observed images.

Each low-resolution frame is a decimated, aliased observation of the true scene. SR is possible only if there are subpixel motions between these low resolution frames, and thus the ill-posed up sampling problem can be better conditioned (Milanfar, 2010). Figure 2.2 shows a simplified diagram describing the basic idea of SR reconstruction. In the imaging process, the camera captures several LR frames, which are downsampled from the HR scene with subpixel shifts between each other. SR construction reverses this process by aligning the LR observations to subpixel accuracy and combining them into a HR image grid (interpolation), thereby overcoming the imaging limitation of the camera.

2.4 The Super Resolution Reconstruction Problem

The super resolution reconstruction problem is to find an estimate of the HR image x from the set of LR images (Vilenna *et al.*, 2012). Therefore, given L LR images y_k, such that $k = 1,...,L$ from the HR images x. the LR images y_k consist of;

$$N = N_h \times N_v \text{ pixels} \qquad 2.1$$

Where N_h and N_v are the observations pixels number in horizontal and vertical respectively and the HR image x of PN pixels, where the integer P > 1 is the factor of increase in resolution. The matrix-vector notation will be adopted such that the LR images y_k and x are arranged as $N \times 1$ and $PN \times 1$ vectors respectively.

The imaging process as presented in Figure 2.2 introduces blurring, warping and downsampling which is modeled as (Vilenna *et al.,* 2012):

$$y_k = AH_kC(S_k)x + n_k = B_k(s_k)x + n_k \qquad 2.2$$

With the system $N \times PN$ matrix,

$$B_k = AH_kC(s_k), \qquad 2.3$$

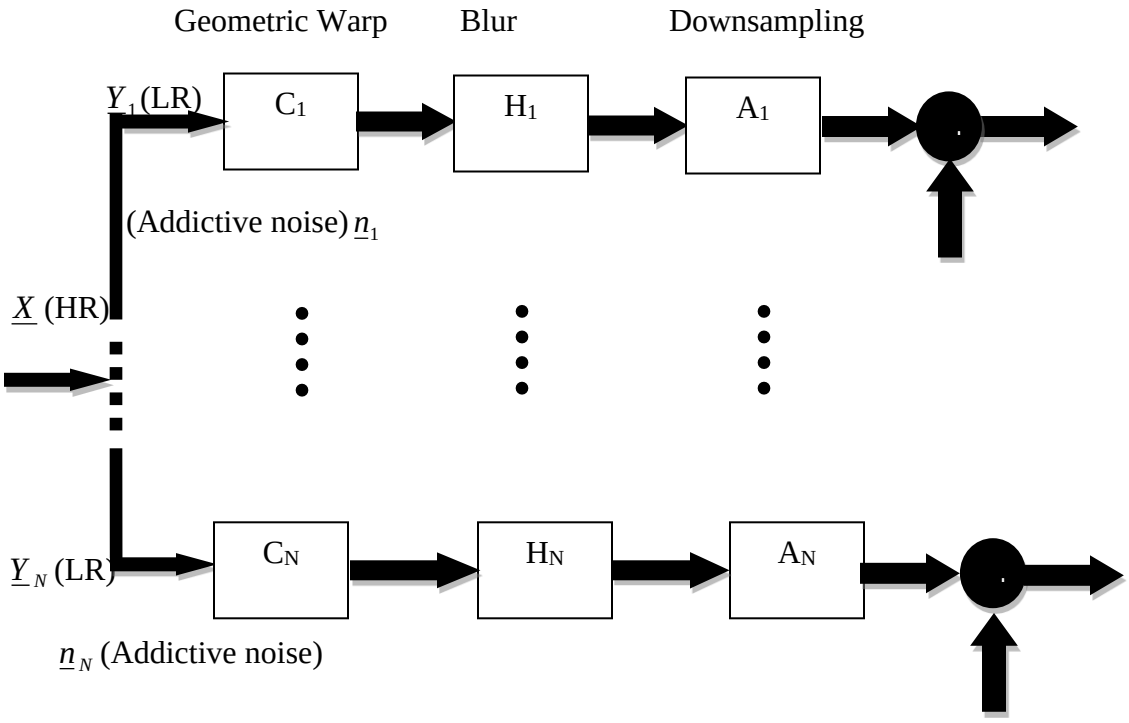

Figure 2.2: The Super Resolution Reconstruction Imaging Process (Vilenna *et al.*, 2012).

where y_k is the measured LR images (noisy, blurry, down-sampled), A is the $N \times PN$ downsampling matrix dictated by the required resolution ration, H_k is the $PN \times PN$ blurring matrix which can be extracted from the camera characteristics, $C(s_k)$ is the $PN \times PN$ warping matrix generated by the motion vector s_k and n_k is the $N \times 1$ acquisition / addictive noise.

However, the matrices H_k, $C(s_k)$ and the noise n_k can be different for each LR image y_k therefore with (Milanfar, 2010):

$$s_k = (\theta_k, c_k, d_k)^t \qquad 2.4$$

where θ_k is the rotation angle, c_k and d_k are the horizontal and vertical translations of the k^{th} HR image with respect to the reference image x, the effects of downsampling, blurring and warping can be combined into a single $N \times PN$ system matrix B_k.

In other words, given Equation (2.2), the super resolution reconstruction problem is to find an estimate of the HR image x from the set of LR image $\{y_k\}$ using prior knowledge about $\{C(s_k)\}, \{n_k\}$ and x.

2.5 Super Resolution Methods

The super resolution methods to be considered in this research work are the Discrete Algebraic Reconstruction Technique DART and Iterative Back Projection technique IBP.

2.5.1 Discrete Algebraic Reconstruction Technique (DART)

Discrete algebraic reconstruction stems from discrete tomography (DT), which is concerned with the problem of recovering images from their projections, where the images are assumed to consist of a small number (2 to 5) of gray values only (Zefreh *et al.*, 2013). Potential benefits of DT are an increase of the reconstruction quality and a reduction of the required number of projection images. The DT reconstruction problem, however, is generally underdetermined and

the number of possible solutions can be substantial. To guide the reconstruction process toward an optimal as well as intuitive solution, the DART algorithm was proposed (Zefreh *et al.*, 2013).

DART allows efficiency in reconstruction of a high-quality image from a limited number of projections. The DART algorithm has been successfully applied to produce accurate reconstructions in several domains such as computed tomography (CT) and electron tomography (Batenburg, Sijbers, Poulsen and Knudsen, 2013). While DART has been applied in CT and electron tomography, the concept of DT has not yet been transferred to the domain of reconstructing an HR image from a set of LR camera images. DART can be applied if the scanned object is known to consist of only a few different compositions, each corresponding to a constant grey value in the reconstruction (Zefreh *et al.*, 2013).

Let $\{y_i\}_i = 1,...,d$ represent a set of d LR images of size $M \times N$. It is assumed that these images are acquired under orthographic projections and that individual scene motions can be modeled as affine transformation. The HR image that is needed to be reconstructed from $\{y_i\}$ is represented by x. Each LR image is modeled as a noisy, uniformly downsampled version of the HR image, which has been shifted and blurred. If D denotes the downsampling operator, G the blurring operator, and A the affine transform that maps the HR grid coordinate system to the LR grid system, this is achieved (Batenburg *et al.*, 2010);

$$DGAx + n = y. \qquad 2.5$$

This can also be rewritten as;

$$Wx + n = y, \qquad 2.6$$

Where $W=GDA$ is the complete system matrix. The reconstruction x is computed on a rectangular pixel array of width w and height h. Hence, the total number of pixels in the reconstruction is given by $n = wh$. For each LR image, we assume that the number of pixels is l. The total number of

available LR pixels is denoted by $m = ld$. The entries of the $n \times 1$ column of vector x correspond to the pixels values of the reconstruction. The $m \times 1$ column vector y contains the LR image pixels, ordered column-wise. The $m \times n$ system matrix W defines the transformation from x to y. Ignoring noise, the reconstruction problem can then be formulated as a system of linear equations (Batenburg *et al.*, 2010);

$$Wx = y \qquad 2.7$$

DART was introduced in the field of CT, where an image needs to be reconstructed from a set of x-ray projection images. DART tries to find a solution to equation 2.7under the constraint that each of the x_i can only take values in a prescribed set. First, a conventional reconstruction is computed. Then, a number of DART iterations are performed, each containing the following steps (Zefreh *et al.*, 2013):

i. The current reconstruction is subdivided into partitions by the thresholding and each of the partitions is assigned the known gray-level value.
ii. The difference between the actual projection data and the forward projection of the segmentation is computed.
iii. Pixels that are on the boundary of a partition are identified.
iv. A regular iterative technique such as Simultaneous Iterative Reconstruction Technique (SIRT) is applied to reconstruct the projection difference in the pixels on the boundaries. The other pixels are kept fixed on the gray level of their partition.

The steps are presented in the algorithm.

Compute a start reconstruction x^0 *using ARM;*
$t := 0$;

While (stop criterion is met) do
begin
$t := t + 1;$
Compute the segmented image $s^t = r\left(x^{t-1}\right);$
Compute the set B^t *of boundary and* I^t *of non-boundary pixels of* s^t *;*
Compute the image y^t *from* x^{t-1} *and* s^t *, setting*
$y_i^t := s_i^t$ *if* $i \in I^t$ *and* $y_i^t := x_i^{t-1}$ *otherwise;*
Using y *as the start solution, compute the ARM reconstruction* x^t *,*
while keeping the pixels in I^t *fixed;*
Apply a smoothing operation to the pixels that are in B^t *;*
End

More formally, in each DART iteration, non-boundary pixels are assigned a given gray level in the prior known set of gray levels. Let *B* be the boundary of the object in the thresholded image, which is defined as the set of all pixels that are adjacent to at least one pixel having a different gray level. Let *I* denote the remaining set of pixels. All pixels in *I* are assigned their thresholded value. The idea of DART is now to exclude the pixels in *I* from the regular Algebraic Reconstruction Method (ARM) iterations and, hence, only update the boundary pixels.

That is, several ARM iterations are performed on the pixels in *B* only. In this way, the number of variables in the linear equation system is significantly reduced, while the number of equations remains the same. In each iteration, the boundary pixels are allowed to vary independently, which may result in large local variations of the pixel values. To regularize the reconstruction algorithm, the boundary pixels are locally smoothed after applying ARM iteration on *B*. Subsequently, the resulting image is again thresholded, a new set of boundary pixels B is determined, and the next ARM iteration is run on the pixels in *B*. These steps are iterated until a certain convergence criterion is met (Van *et al*. 2010).

Figure 2.3 shows the block diagram of DART. A continuous reconstruction is computed as a starting point, using the ARM. Subsequently, a number of DART iterations are performed.

Reconstructing the binary image from Figure 2.4(a) from only 12 projections it is assumed that the two grey levels (black and white) are known in advance. The continuous Simultaneous Algebraic Reconstruction Technique (SART algorithm is chosen as the ARM. Figure 2.4(b) shows the ARM reconstruction after 10 iterations. From the reconstructed image in Figure 2.4(b), it is difficult to decide where the edges of the object are exactly.

The thresholded reconstruction in Figure 2.4(c) shows that looking only at the interior of the object that is not too close to the boundary, the pixels in the thresholded image have the right grey level. The same holds for pixels in the background region that are far away from the object boundary. Next, the boundary region B of the object is located in the thresholded image, which is defined as the set of all pixels that are adjacent to at least one pixel having a different grey level. The boundary is shown in Figure 2.4(d).

Going back to the original grey level ARM reconstruction, all pixels that are not in B are assigned their thresholded value, either black or white. Next, several ARM iterations are performed again, while keeping the pixels that are not in B fixed at the assigned threshold values. That is, the only pixels that are updated by ARM are the pixels in B. In this way, the number of variables in the linear equation system is vastly reduced, while the number of equations remains the same.

The result of the boundary reconstruction after one ARM iteration is shown in Figure 2.4(e), where the gray levels have been scaled to show the range of gray levels present in the boundary pixels. In regions of the boundary where too many white pixels have been fixed, the surrounding boundary pixels have strongly negative pixel values, to compensate. The opposite

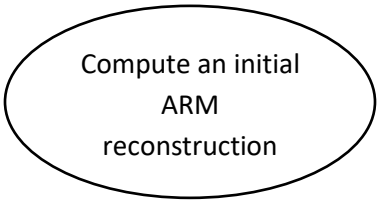

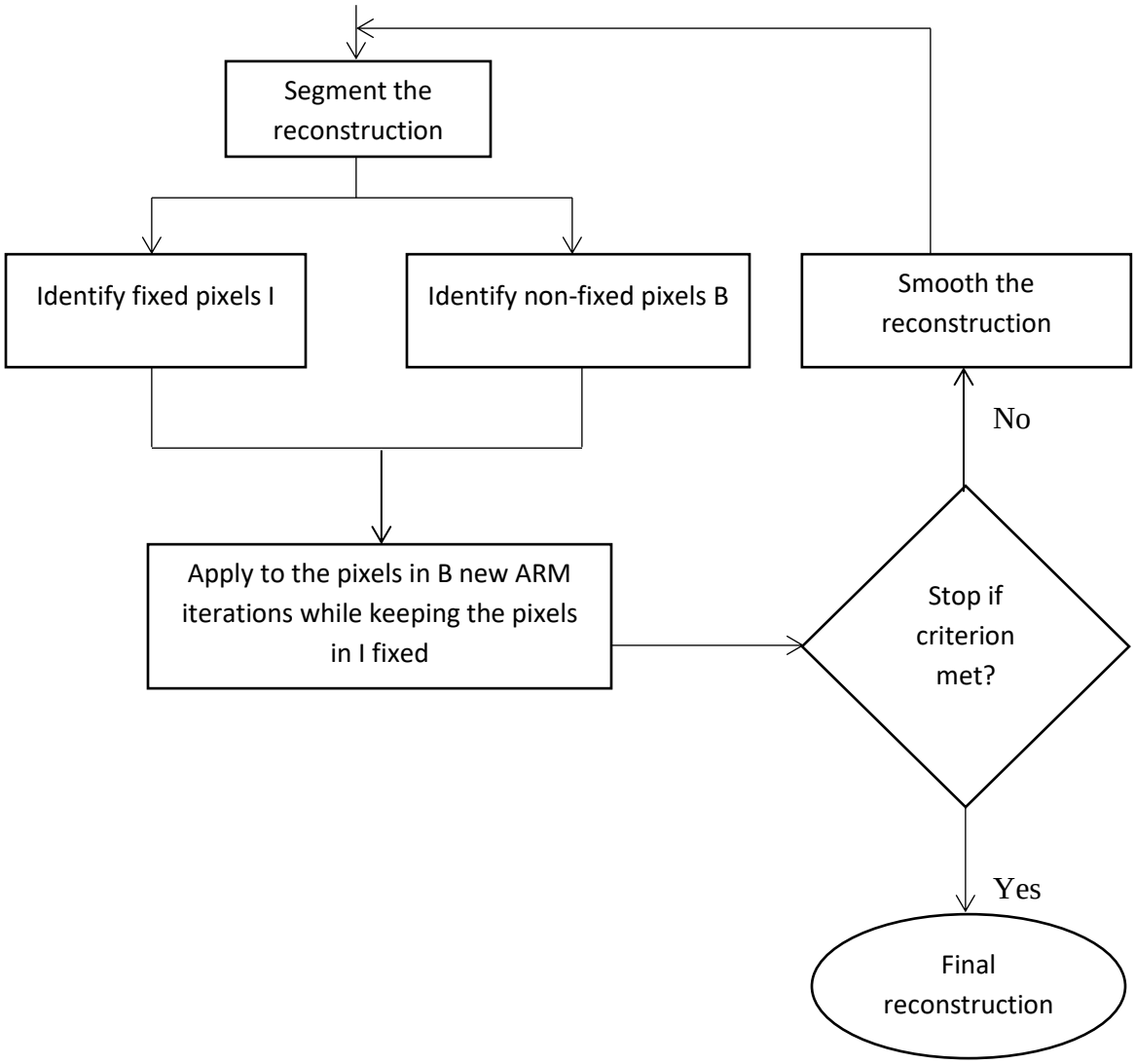

Figure 2.3: Flow Diagram of the DART Algorithm (Zefreh *et al.*, 2013)

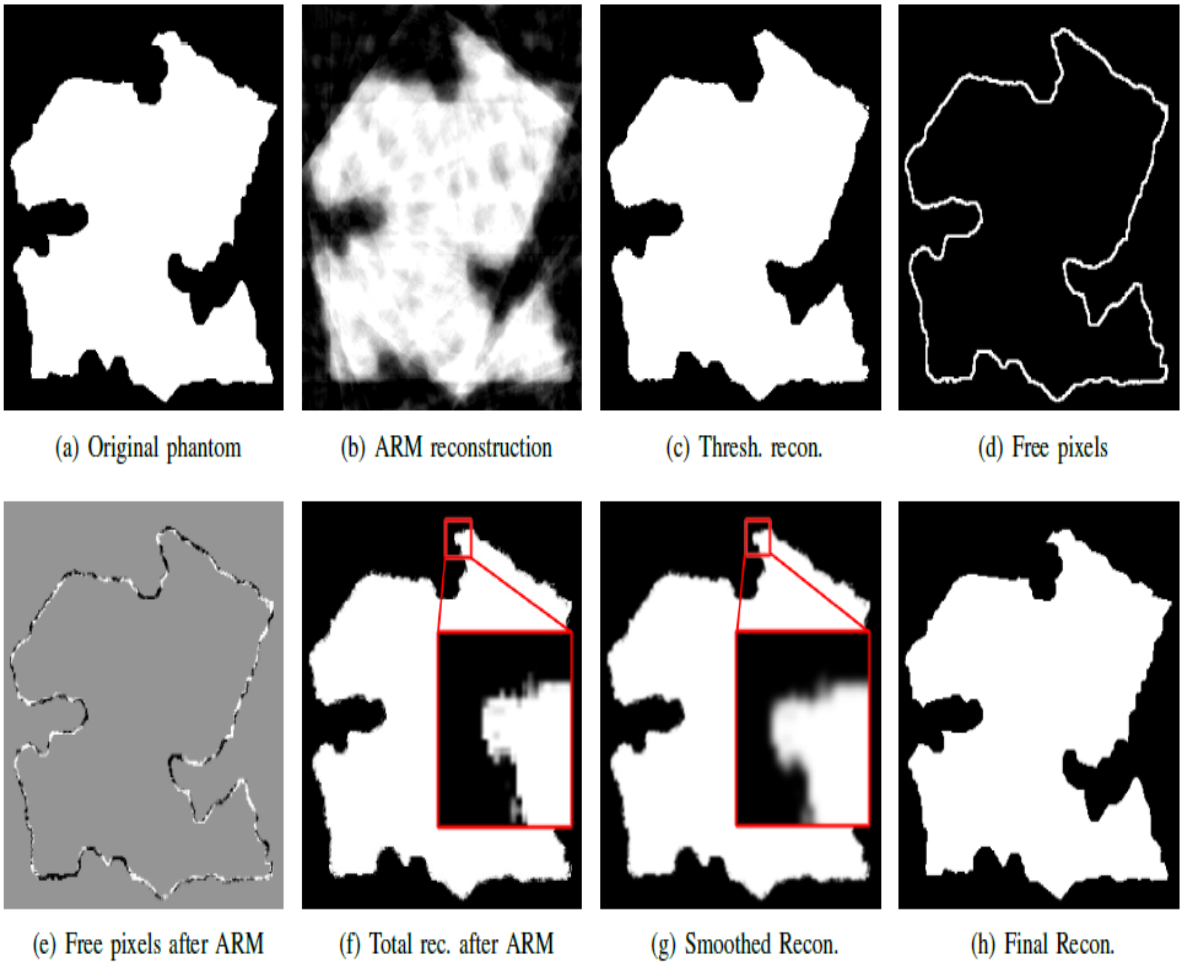

Figure 2.4: The Reconstruction of a Phantom (Batenburg *et al.*, 2013).

occurs at parts of the boundary where the extent of the background has been overestimated in the first thresholded ARM reconstruction. In this way, the values of the boundary pixels indicate how the boundary should be adapted in a new estimate of the object. Figure 2.4(f) shows the complete reconstruction obtained by merging the boundary with the fixed interior and background.

In the ARM step, each of the boundary pixels is allowed to vary independently, which may result in large local variations of the pixel values. In experiments, it is observed that smoothing must be applied to the boundary after the ARM step. Figure 2.4(g) shows the result of this smoothing operation. This completes the DART iteration. Subsequently, a thresholded version of the image is computed again, and each of the steps just described is repeated iteratively. As a consequence of the boundary update step, the set of boundary pixels will change between subsequent iterations, allowing for movement of the object boundary. The final result of this procedure, after four iterations, is shown in Figure 2.4(h). It is nearly identical to the original phantom image.

2.5.2 Iterative Back Projection (IBP)

IBP technique was first proposed by Irani *and* Peleg (1993), it can attain the High Resolution image interpolation and de-blurring simultaneously, while its motto is that the reconstructed HR image from the degraded Low Resolution image should produce the same observed LR image if passing it through the same blurring and down-sampling process. The IBP technique can minimize the reconstruction error by iteratively back-projecting the reconstruction error into the reconstructed image. IBP is a classical SR method with low computational complexity that can be applied in real time applications (Fan, Gan, Qiu and Zhu, 2011).

IBP is an efficient algorithm to acquire the HR image by minimizing the norm of the reconstruction error (Marcia, Aguena, Nelson and Mascarenhas, 2011; Siddique, 2012). With the help of given an estimate of the reconstructed HR image and a model of the imaging process, a set of simulated LR images can be generated. Each simulated LR image is compared with the actual version and then the error can be used for correcting the estimated image. In fact, it is difficult to restore a HR image in a one-shot manner. Therefore, an iterative procedure is needed. This process

is iterated until some stopping condition is achieved. Generally, the minimization of some error criterion between the simulated and observed LR images is adopted as the stopping condition (Lin and Lai, 2008).

This method begins with an image registration procedure and iteratively refines the simulated low resolution images by subtracting the observed images from them. First it finds a rough estimation of high resolution (HR) image called as "initial guess" $X^0$and iteratively a "gradient" image is added to it during the course of operation. The gradient image that is calculated from the sum of the errors between each LR image and the estimated HR image (Irani and Peleg, 1991) is given as,

$$Gradientimage = (y - y^{sim}) \quad 2.8$$

Where, y= Observed LR images

y^{sim}= Simulated LR images

These simulated LR images are compared with the observed ones and the error generated between them is back projected onto the initial guess after multiplying it with the back projection operator,

$$X = X^0 + A^{bp}(y - y^{sim}) \quad 2.9$$

Where, A^{bp}= back projection operator calculated from the imaging process

X^0= Initial guess

X= Output High Resolution image

The algorithm considers translational, rotational, blur and down-sample operator in the back projection matrix.

The IBP technique here successfully solves the problem of blur and noise, still due to ill-posed nature of the inverse problem, the technique fails to generate a unique solution. The multi-

modal optimization technique helps here in finding the more appropriate solution of X, because Iterative Back Projection technique being an inverse problem provides no unique solution. Therefore need of search technique to find the best solution where the mean square error of the reconstructed image is minimized.

IBP is an efficient method that is repeated iteratively to minimize the energy of the error. The method can be used to incorporate constraints, such as smoothness or any other additional constraint which represents a desired property of the solution. Figure 2.5 shows a simple block diagram of IBP. In IBP approach, process starts with the input LR image. The initial HR image can be generated from the input LR image by decimating the pixels. The initial HR image is degraded and down sampled to generate the observed LR image. The simulated LR image is subtracted from the observed LR image.

The HR image is estimated by high pass filter for edge projection and back projecting the error (difference) between simulated LR image and the observed LR image. This process is repeated iteratively to minimize the energy of the error. This iterative process of SR does iterations for some predefined iterations (Rujul and Nita, 2013). Mathematically, the SR steps according to IBP are written as (Patel, 2013):

$$X^{(n+1)} = X^{(n)} + X_e + HPF(X^{(0)}) \qquad 2.10$$

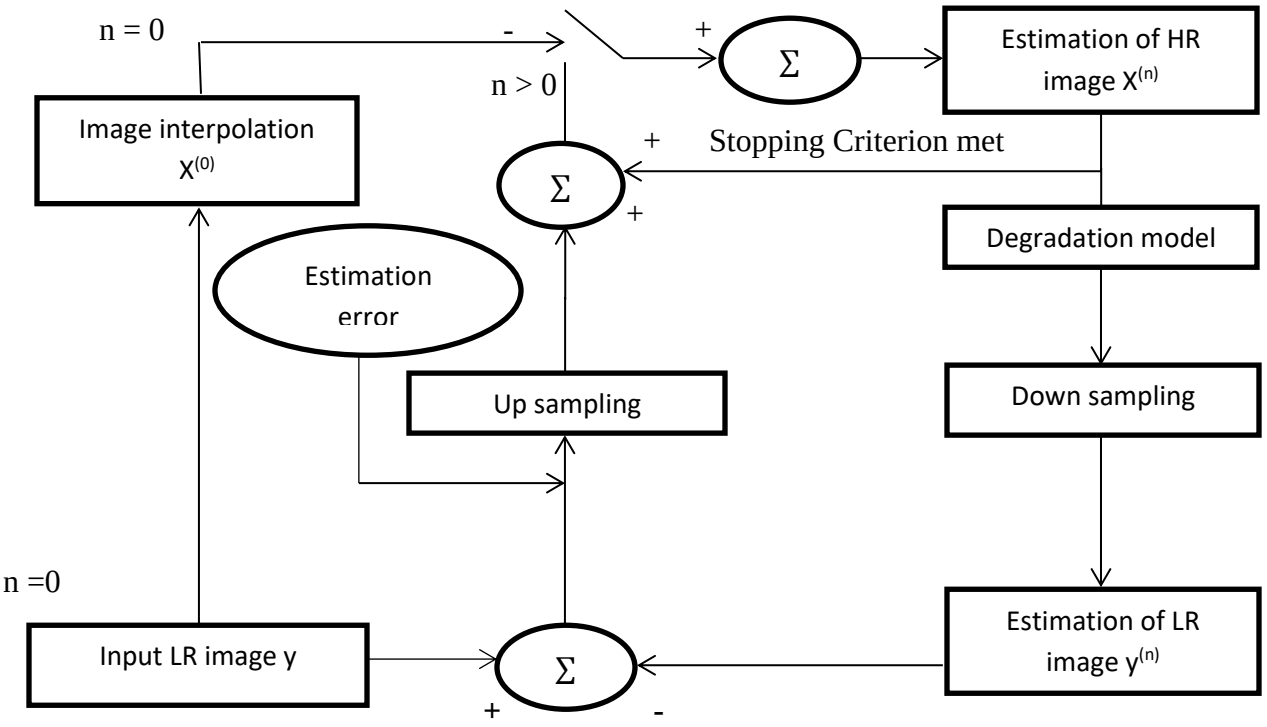

Figure 2.5: A Simple Block Diagram of the IBP algorithm (Rujul and Nita, 2013)

Where, $X^{(n+1)}$ is estimated HR image of n+1th iteration; $X^{(n)}$ is estimated HR image of n^{th} iteration; X_e is error correction and HPF($X^{(0)}$) is the high pass filter for the image $X^{(0)}$ that is obtained from the interpolation of initial LR image.

In IBP method, to generate the simulated LR image, the estimated HR image needs to be down sampled. Due to down-sampling procedure, sampling frequency is decreased that generates distortions in high frequency components and the aliasing problem (Wang, Liang, Chang and

Chang, 2009). Therefore, the HR image obtained from High Pass filter needs to be further filtered by a Gaussian filter to eliminate the distortions from the down sampling procedure. As a result, the updating procedure can be summarized as mathematical equation by following two steps iteratively (Rujul and Nita, 2013):

i. Compute the error from LR images as

$$X_e = (y - y^{(n)}) \uparrow s \qquad 2.11$$

Where, $\uparrow s$ is upsampling; y is initial input LR image; $y^{(n)}$ is simulated LR image of n^{th} iteration; X_e is error estimation.

ii. Estimation of the simulated LR image is given as

$$y^{(n)} = (X^{(n)} * W) \downarrow s \qquad 2.12$$

Where, $\downarrow s$ is downsampling; $y^{(n)}$ is simulated LR image of n^{th} iteration; W is degradation function; $X^{(n)}$ is estimated HR image of n^{th} iteration. Update the HR image by back-projecting the error X_e, as equation (2.10). Table 2.1 shows the overall advantage of IBP and DART.

Table 2.1: Overall advantages of IBP and DART Super Resolution Reconstruction Technique

Iterative Back Projection	Discrete Algebraic reconstruction Technique
It is very efficient for minimizing reconstruction error	It provides noise removing information and additional edge smoothing priorities
It helps to realize better and more reliable visual quality of super resolved images	It makes use of minimal LR images in reconstruction of images
It is computationally time efficient.	It is computationally optimal

2.6 Sampling Theorem

Sampling leads to periodicity in frequency domain (Oppenheim and Schafer, 2010). The sampling theorem defines the conditions for successful sampling of particular interest being the minimum rate at which samples must be taken. The sampling theorem shows that a continuous time

band-limited signal may be represented perfectly by its samples at uniform intervals of T seconds if T is small enough. In order words, the continuous time signal may be reconstructed perfectly from its samples; sampling at a high enough rate is information-lossless. The sampling theorem places restrictions on the frequency content of the time function signal, f(t), and can be simply stated as follows: in order to recover the signal function f(t) exactly, it is necessary to sample f(t) at a rate greater than twice its highest frequency component (Bernard and Gernot, 2013).

If the Fourier transform F(w) of a signal function f(t) is zero for all frequencies above $|w| \geq Wc,$ then f(t) can be uniquely determined from its sampled values $fn = f(nT).$ these values are a sequence of equidistant sample points spaced $\frac{1}{2fc} = \frac{T_c}{2} = T$ apart. $f(t)$ is thus given by Bernhard and Gernot, (2013) as:

$$f(t) = \sum_{n=-\infty}^{\infty} f(nT) \frac{\sin \omega_c (t - nT)}{\omega_c (t - nT)} \qquad 2.13$$

For example, to sample an analog signal having a maximum frequency of 2Kc requires sampling at greater than 4Kc to preserve and recover the waveform exactly.

2.6.1 Downsampling

In signal processing, downsampling is the process of reducing the sampling rate of a signal (Proakis, 2000). This is usually done to reduce the data rate or size of the data. The downsampling factor is usually an integer or a rational fraction greater than one. This factor multiplies the sampling time or, equivalently, divides the sampling rate. Downsampling by an integer factor, M, can be explained as a 2-step process, with equivalent implementation that is more efficient to (Bernhard and Gernot, 2013):

i. Reduce high-frequency components with a digital low pass filter

ii. Decimate the output sequence, keeping only every M^{th} output sample.

Downsampling amounts to scaling of time axis by a factor of 1/N where N is the number of impulse sequence samples (Proakis, 2000). Decimation causes high-frequency signal components to be misinterpreted by subsequent users of the data, which is a form of distortion called aliasing. When downsampling by a rational fraction where M/L denote the downsampling factor and M>L, M is the downsampling factor and L is the upsampling factor.

While upsampling requires a low pass filter after increasing the data rate, downsampling requires a low pass filter before decimation. Therefore, both operations can be accomplished by a single filter with the lower of two cutoff frequencies. For the M > L case, the anti-aliasing filer cutoff, $\frac{0.5}{M}$ cycles per intermediate sample, is the lower frequency.

2.6.2 Upsampling

Upsampling is the process of increasing the sampling rate of a signal by adding N-1 zero samples between every sample of the input where N is the total number of samples (Bernhard and Gernot, 2013). It effectively scales time axis by factor N, filters the resulting sequence in order to create a smoothly varying set of sequence samples which leads to interpolation between the non-zero samples of the resulting sequence. Interpolation filter removes all replicas of the signal transform except for the baseband copy.

2.6.3 Aliasing

Aliasing occurs when a system is measured at an insufficient sampling rate (Bernhard and Gernot, 2013). It is the overlap of replicated signals in frequency domain. Therefore, it is important to suppress such components to an acceptable level of distortion using a lowpass filter called an

anti-aliasing filter. Given periodic frequency distribution of a sampled function x (t) with Fourier transform X(f), aliasing occurs when adjacent copies of X(f) overlap. This concept results in a frequency mistakenly taking on the identity of an entirely different frequency when recovered. On the surface, it is easily said that anti-aliasing designs can be achieved by sampling at a rate greater than twice the maximum frequency found within the signal to be sampled (Proakis, 2000). Analog signals are usually low-pass filtered to remove most or all of the components above the Nyquist frequency in order to avoid aliasing.

The purpose of the anti-aliasing filter is to ensure that the reduced periodicity does not create overlap. The condition that ensures the copies of X(f) do not overlap each other is B < $\frac{1}{M}.\frac{1}{2T}$, where T is the interval between samples, $\frac{1}{T}$ is the sample rate, M is the decimation factor, B is the anti-aliasing filter with a cutoff frequency less than $\frac{1}{M}$ multiplied by the Nyquist frequency and $\frac{1}{2T}$ is the Nyquist frequency (Oppenheim and Schafer, 2010).

2.7 Review of Related Works

High resolution (HR) images are very useful in different areas of life and are very applicable in areas like security, health to mention a few. Various researchers have explored the area of super resolution over the years using various methods.

Weisheng *et al.* (2009) incorporated adaptively the non-local iterative back projection (NLIBP) algorithm into the IBP process so that the reconstruction errors can be reduced during image enlargement. The IBP technique iteratively reconstructs a HR image from its blurred and downsampled LR counterpart. However, the conventional IBP method often produced many jaggy and ringing artifacts because the reconstruction errors are projected into the reconstructed image isotopically. One major drawback of this approach is that it suffers from non-edge guidance.

Van *et al*. (2010) developed a discrete tomography approach for super resolution micro-CT images: application to bone. The authors upsampled the reconstruction grid combined with DART algorithm in which the scanned objects are assumed to be composed of homogeneous materials. Their results show that the method generates reconstructions with significantly more details compared to conventional reconstruction algorithms. However, the method still suffers from optimality because the method used is not highly optimal for super resolution reconstruction.

Zefreh *et al*. (2013) developed a discrete algebraic reconstruction technique: a new approach for super resolution reconstruction of license plates. The researchers used DART to reconstruct a high resolution license plate from a set of low resolution camera images. The simulation and result shows that DART algorithm combines the efficiency of iterative algebraic methods from continuous tomography with the power of discrete algebraic reconstruction algorithm to compute an accurate HR image from a small number of LR images. However, it gave a PSNR, SSIM and MSE of 81.229dB, 0.9989 and 0.007 respectively.

Monalisa (2013) introduced spatial super resolution based image reconstruction using IBP and evolutionary method. The author used IBP along with evolutionary technique for optimization. Three lacunae of LR images were considered in the thesis that is, relative motion between scene and camera, sensor blur and down-sampling during image acquisition. The optimization algorithm used is Cuckoo optimization algorithm with levy flights. The results show that the images were of a higher quality than when just IBP is used but the edge information of the images are still noisy and this method is not effective for resolution enhancement for videos. It also gave an average PSNR, SSIM and MSE of 28.903, 0.9999 and 0.00515 respectively.

Rujul and Nita (2013) researched on effective novel single image super resolution approach to recover a high resolution image from a single low resolution input image. The approach is based

on IBP combined with the canny edge detection and Gabor filter to recover high frequency information. It was applied on different natural gray images and compared with different existing image super resolution approaches. The results showed that the algorithms can more accurately enlarge the low resolution image than previous approaches and it is robust to noise with edge preservation. However, canny edge detection does not incorporate additional image prior model that guides and helps realize better super resolved image. As a result it is not reliable and efficient for highly degraded images.

Patel (2013) addressed the problem of recovering a super resolved image from a single low resolution input. The technique is based on combining IBP method with the edge preserving Infinite Symmetrical Exponential Filter (ISEF). The method was applied on different type of images including face images, natural images and medical images; the performance was compared with a number of other algorithms, bilinear interpolation and nearest neighbor interpolation. The method showed marginal superiority to the existing method in terms of visual quality and PSNR. It gave an average PSNR, SSIM and MSE of 33.89, 0.9250 and 0.17765 respectively.

Lin (2014) developed an iterative back projection super resolution algorithm for low resolution image upsampling. A super resolution (SR) algorithm based on an iterative back project interpolation was proposed to obtain more reliable information in the edge area. For evaluation of the performance, the PSNR and the SSIM criteria of the proposed algorithm were compared with those of other methods. The experimental results of 28.743 dB in average PSNR and the 0.9165 in average SSIM show the superiority of the method. Furthermore, the computational complexity of the algorithm was reduced while maintaining similar image quality. However, it is computationally complex.

Fagbola (2015) developed a pose illumination invariant feature extraction technique for low resolution video feeds. IBP-MAP was developed using edge and non-edge details in Maximum A Posterior (MAP) priors. Resulting reconstruction error was estimated, minimized and back-projected by Iterative Back Projection (IBP). LDA-LBP-GWT was developed by fusing the facial features of Linear Discriminant Analysis (LDA), Local Binary Pattern (LBP) and Gabor Wavelet Transform (GWT) into a Single Feature Set (SFS). The SFS was optimized using particle swarm algorithm. The developed IBP-MAP technique produced PSNR of 33.77dB, ISNR of 11.82dB and NI of 34.00 and the developed LDA-LBP-GWT produced FA of 725, RA of 63.75%, RT of 103.65s and FR of 0.

From the review of related works, it is discovered that various techniques had been used by researchers for super resolution to achieve high resolution images. However, none of the study have experimented IBP with DART to ascertain the possible outcome.

CHAPTER THREE

METHODOLOGY

3.1 The Developed Discrete Algebraic Back Projection Reconstruction Technique for Low Resolution Images

The developed discrete algebraic back projection super resolution technique for low resolution images is made up of three distinct stages which include:

i. Image dataset acquisition.

ii. Design of the proposed Discrete Algebraic Back Projection reconstruction technique.

iii. Implementation of the proposed Discrete Algebraic Back Projection super resolution technique for image reconstruction.

The conceptual diagram for the developed discrete algebraic back projection technique is presented in Figure 3.1.

3.1.1 Image dataset acquisition

The first step in this research work involved image acquisition. The database of the images used in this research was acquired using a digital camera of a resolution size of 5mp (megapixel). Images were acquired in BMP, JPEG, GIF, PNG or TIFF format. This is to ascertain that an image acquired from a regular imaging device can be reconstructed. The images are kept in a file which was imported into the system one after the other as needed.

3.1.2 Design of the developed DABPRT technique

A super resolution reconstruction technique based on the combination of Discrete Algebraic Reconstruction Technique (DART) and Iterative Back Projection (IBP) was designed to address the low resolution challenges in images. DART was used to increase the reconstruction quality and reduce the required number of projection images. DART allows

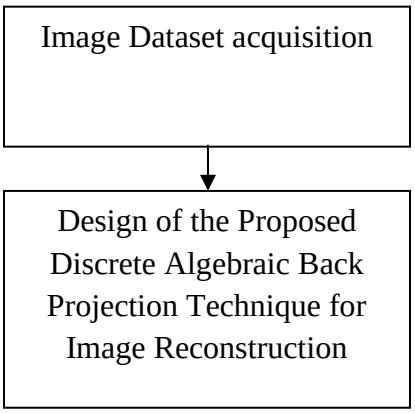

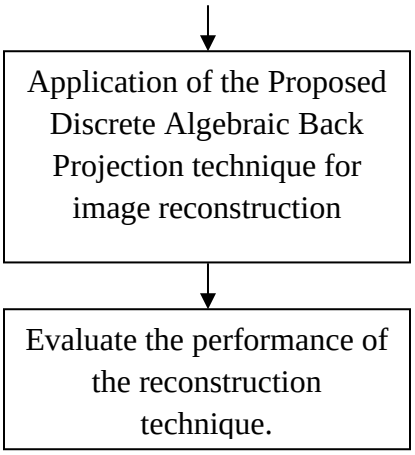

Figure 3.1: Conceptual Diagram of the Developed Discrete Algebraic Back Projection Reconstruction Technique for low resolution Images

reconstruction of high quality images from a limited number of projections. DART was used on the image and it gave an output estimate which was then used as the initial guess in IBP which was introduced to minimize the reconstruction error produced by DART in an iterative manner and help to achieve a better and more reliable super resolved images.

The Block diagram of the developed Discrete Algebraic Back Projection reconstruction technique is presented in Figure 3.2. It is made up of eight (8) major components, which are low resolution images, image interpolation, image upsampling process, image downsampling process, image degradation model, the DART, estimated low resolution image and the estimated high

resolution image. The process starts with the input LR image which was magnified through image interpolation.

The initial HR image was degraded and downsampled to generate observed LR image, Equation 2.1 was used when appropriate. The simulated LR image was subtracted from the observed LR image to obtain the reconstruction error. The DART served as high pass filter which added extra high frequency information to the up-sampled images from initial and simulated LR images. In the iterative process, the estimated low resolution images was interpolated and reconstructed to obtain an estimated HR image while the reconstruction error was back projected to the estimated HR image.

The Activity Diagram of the developed technique is presented in Figure 3.3. The number of iterations needed for the reconstruction of the image is set so also the parameters for degrading the image which are max displacement, angle of variation, Noise and blurring. The image is then loaded from a dedicated file and the number of low resolution images to be used are set and created then DART is applied to get an output estimate which is then inputted into IBP to reduce the reconstruction error produced by DART and the output gives a resolved image.

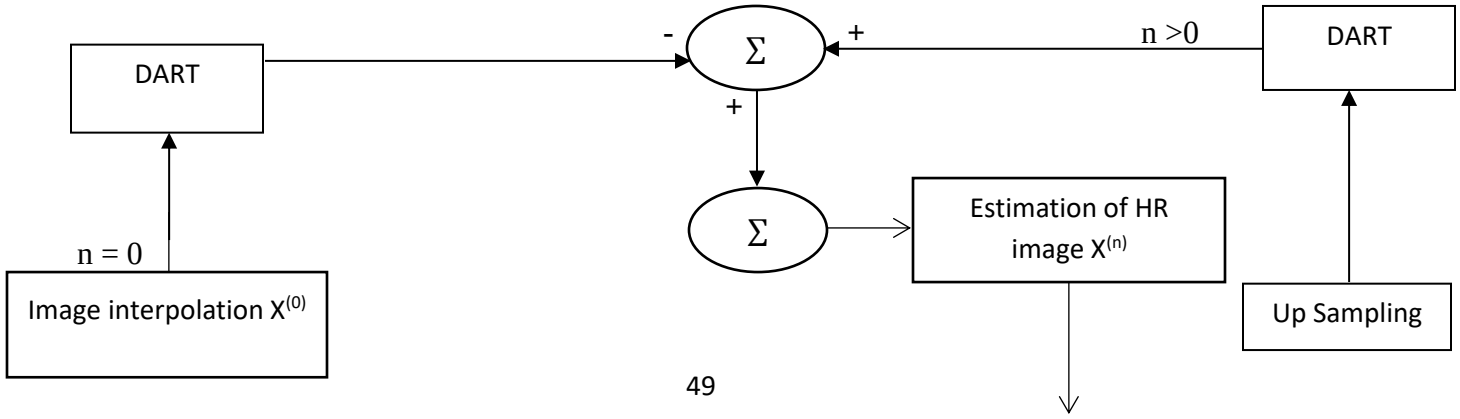

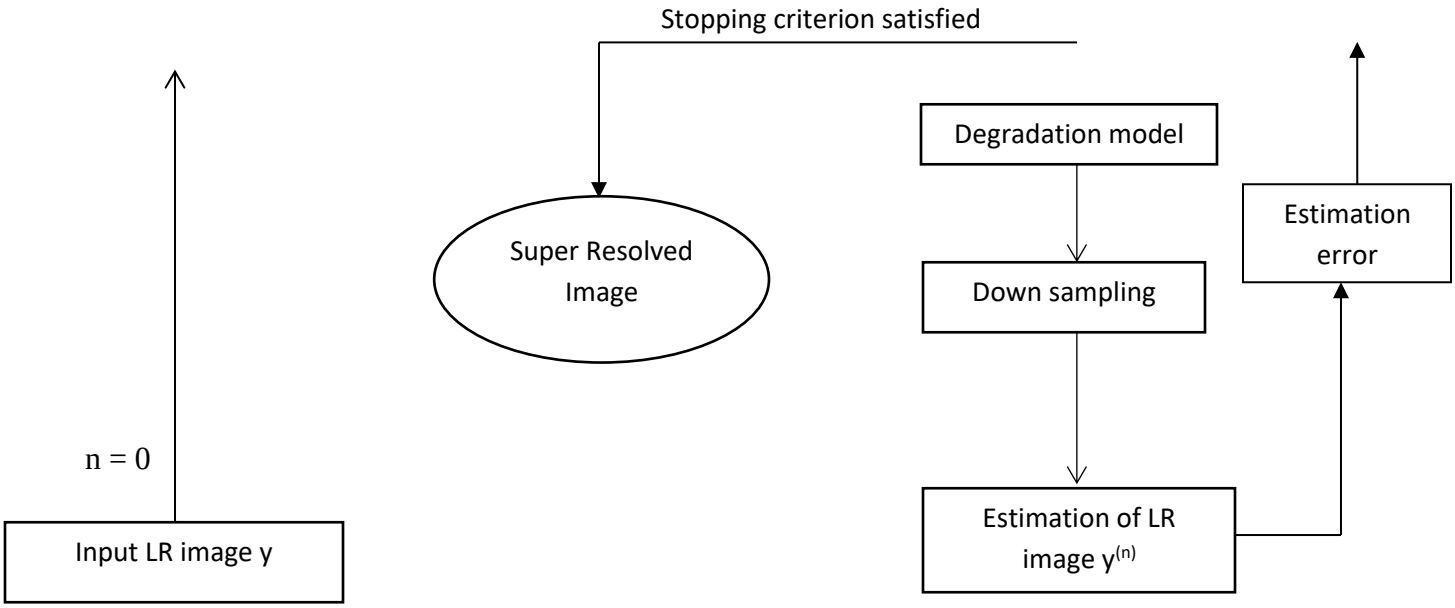

Figure 3.2: The Block Diagram of the Developed Discrete Algebraic Back Projection Reconstruction Technique

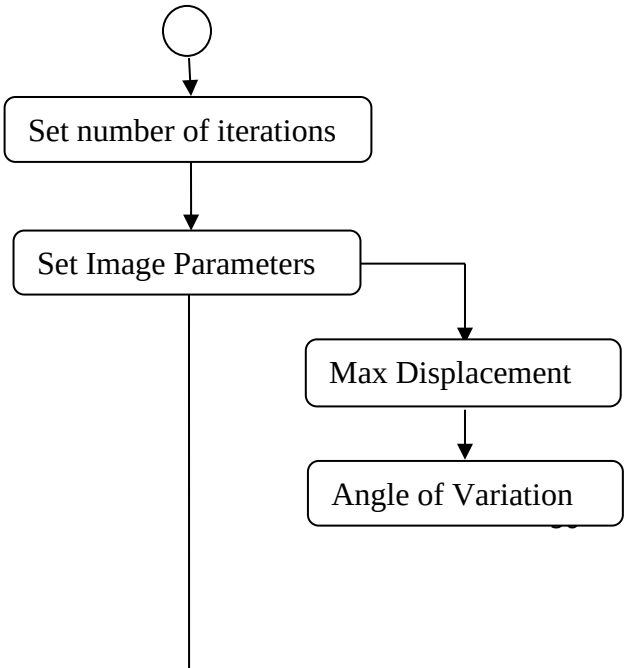

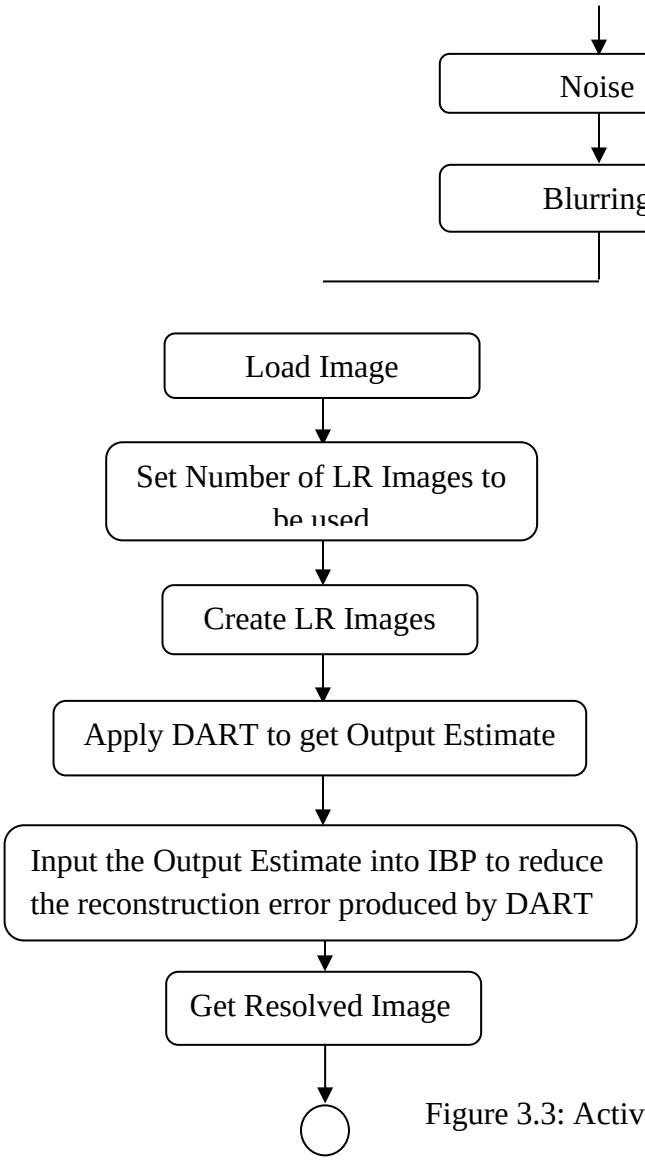

Figure 3.3: Activity Diagram of the Developed DABPRT Technique

3.1.3 The implementation of the developed technique

The implementation of this research was done in MATLAB environment. This is because MATLAB is very powerful in computing system for handling the calculations involved in scientific and engineering problems and MATLAB has a rich set of toolboxes which allows breaking down of many complex problems. MATLAB stands for MATrix LABoratory. The image processing function, math and some user-defined functions and toolbox will be adopted in this research.

A general structure of the developed Discrete Algebraic Back Projection Reconstruction Technique (DABPRT) is presented in Figure 3.4. From a set of LR images created, $y^{(1)} \ldots y^{(n)}$, an estimated high resolution image *y* was obtained using the developed SRR technique.

3.2 Performance Evaluation

The total of 50 LR images was used in this research. The metrics that were used to evaluate the performance of the algorithm are Mean Square Error (MSE), Peak Signal to Noise Ratio (PSNR) and Structural Similarity (SSIM) because they are the basic metrics to evaluate images.

i. Mean Square Error is defined as:

$$MSE = \frac{\sigma^2}{m} \qquad 3.1$$

where σ is the standard deviation standard being estimated and m is the sample size

ii. Peak Signal to Noise Ratio (PSNR) is defined as:

$$PSNR = 10 \log_{10} \left(\frac{2^2}{MSE} \right) \qquad 3.2$$

where MSE is Mean Square Error

$y^{(1)}$

The Developed Super Resolution Reconstruction Technique

Figure 3.4: General Structure of the Developed Super Resolution Reconstruction Technique

iii. Structural Similarity (SSIM) is defined as:

$$SSIM(x,y) = \frac{(2\mu_x\mu_y + c_1)(2\sigma_{xy} + c_2)}{(\mu_x^2 + \mu_y^2 + c_1)(\sigma_x^2 + \sigma_y^2 + c_2)} \quad 3.3$$

where μ_x is the average of x;

μ_y is the average of y;

σ_x^2 is the variance of x;

σ_y^2 is the variance of y;

σ_{xy} is the covariance of x and y;

$c_1 = (k_1 L)^2$ and $c_2 = (k_2 L)^2$ which is the variables to stabilize the division with weak denomination;

where L is the dynamic range of the pixel values;

$k_1 = 0.01$ and $k_2 = 0.03$ by default.

CHAPTER FOUR

RESULTS AND DISCUSSION

4.1 Results of the Developed Discrete Algebraic Back Projection Technique

The result of the developed Discrete Algebraic Back Projection Reconstruction Technique (DABPRT) was implemented using MATLAB 8.0 (2012a) on windows 7 64-bit operating system, TOSHIBA with Celeron ® Dual Core Central Processing Unit (CPU) with a speed of 2.10GHz, 4GB Random Access Memory (RAM) and 465GB hard disk drive. The source codes for the

DART, IBP and DABPRT algorithms and the graphics user interfaces are presented in Appendix A, B and C. The low resolution images used were acquired using *vivicam* digital camera of 5.0 Mega Pixels (MP) and a total of 50 images were used in this research work. The images were acquired in JPEG format.

A Graphical User Interface (GUI) - oriented application was developed to obtain results for IBP, DART and the developed DABPRT techniques after reconstructing the images acquired. Figure 4.1 shows a sample of the application's GUI.

The GUI is divided into eleven (11) panels:

i. Number of Iterations: This panel allows the user to choose the number of iterations to be done on an image to be reconstructed.

ii. Maximum Displacement: This panel introduced a displacement to the original image hereby, degrading the image.

iii. Rotation: This panel introduced rotation or tilt to the image furthering the degradation of the image.

iv. Noise: This panel introduces noise to the original image.

v. Blurring Standard deviation: This panel introduces blur to the image.

vi. Load Image: This panel allows the user to load or call an image from a specific or dedicated folder.

vii. Select Number of Low Resolution to use: This panel allows users to select the number of low resolution images to be created to use in the reconstruction of the degraded image. This panel gives a maximum of 10 numbers.

viii. Create Low Resolution Images: this panel creates the low resolution images.

ix. Apply IBP: This panel allows the user to apply IBP to the image for reconstruction. It gives a reconstructed image and result in form of PSNR, SSIM and MSE.

x. Apply DART: This panel allows the user to apply DART to reconstruct the degraded image. It gives results in the form of PSNR, SSIM and MSE.

xi. Apply DABPRT: This panel allows the user to apply the developed technique to reconstruct low resolution images. It also gives result in form of PSNR, SSIM and MSE which can be compared to that of IBP and DART.

The images were subjected to Equation 2.1 to generate the low resolution images for the reconstruction process where appropriate and Equation 2.2 is applied to introduce blurring to the image, so also Equation 2.4 is used to introduce noise to the image where appropriate. The image quality is determined by PSNR, SSIM and MSE. A good reconstruction algorithm generally gives low value of MSE and high value of PSNR and SSIM. Therefore, in this research work, PSNR, SSIM and MSE were obtained for IBP, DART and the developed DABPRT resolution reconstruction techniques.

Figure 4.1: A sample of the DABPRT GUI

4.2 Results Obtained on Implementation of the Developed DABPRT Technique

The result obtained from the reconstruction of low resolution images using IBP, DART and DABPRT are presented in Tables (4.1, 4.2, 4.3 and 4.4) respectively. In all the evaluations carried out, the PSNR, SSIM and MSE were reported. For image 1, 10 iterations was selected, 10 numbers maximum displacement, rotation angle of 45^{o}, noise variance of 0.4 and blurring standard deviation of 0.4 with 4 number of LR images created, the result is shown in Table 4.1. For image 2, 8 iterations were made, 14 number maximum displacement was selected, 27^{o} rotation angle, 0.6 noise variance and 0.3 blurring standard deviation with 5 number of LR images created, the result is shown in Table 4.2.

Image 3 was reconstructed with 12 numbers of iterations, 14 number maximum displacement, 54^{o} rotation angle, 0.2 noise variance and blurring standard deviation of 0.6 with 7 LR images created, the results are shown in Table 4.3 while image 4 was reconstructed with 9 iterations, 8 maximum displacement, rotation angle of 36^{o}, noise variance of 0.3 and 0.7 blurring standard deviation with 4 LR images created, the result is shown in Table 4.4.

4.2.1 Peak Signal to Noise Ratio (PSNR)

Table 4.1 shows the performance evaluation results of the SRR method for image 1. The PSNR of IBP, DART and the developed DABPRT measured in decibel (dB) are 77.14, 71.99 and 80.15 respectively. This reveals that the developed DABPRT produced the highest PSNR, followed by IBP and DART in that order. In Table 4.2, the result for image 2 is presented; the PSNR of IBP, DART and DABPRT are 84.45, 73.19 and 87.4566 respectively.

A similar trend was presented in Table 4.3 with the result of IBP, DART and DABPRT are 91.89, 72.74 and 94.90 respectively, so also in Table 4.4 with PSNR of IBP, DART and DABPRT are 76.22, 68.87 and 79.22 respectively. By implication, the developed DABPRT

Table 4.1 Performance Evaluation Results of the SRR Techniques for Image 1

SRR Techniques	PSNR	SSIM	MSE
IBP	77.14	1	0.00125525
DART	71.99	1	0.0041473
Developed DABPRT	80.15	1	0.000627627

Table 4.2 Performance Evaluation Results of the SRR Techniques for Image 2

SRR Techniques	PSNR	SSIM	MSE
IBP	84.45	1	0.000233589
DART	73.19	1	0.00311425
Developed DABPRT	87.46	1	0.000116794

Table 4.3 Performance Evaluation Results of the SRR Techniques for Image 3

SRR Techniques	PSNR	SSIM	MSE
IBP	91.89	1	0.0000420886
DART	72.74	1	0.00345648
Developed DABPRT	94.90	1	0.0000210443

Table 4.4 Performance Evaluation Results of the SRR Techniques for Image 4

SRR Techniques	PSNR	SSIM	MSE
IBP	76.22	1	0.00155289
DART	68.87	1	0.00843556
Developed DABPRT	79.23	1	0.00077645

shows significant improvement over IBP and DART in terms of visual quality, thereby, produced a super-resolved image with better visual quality than IBP and DART.

4.2.2 Mean Square Error (MSE)

To evaluate the error from the techniques used, Mean Square Error is used. The lower the mean square error, the better the technique. From Table 4.1, MSE for IBP, DART and DABPRT are 0.00125525, 0.0041473 and 0.000627627 respectively. Likewise Table 4.2 shows that the MSE for IBP, DART and DABPRT as 0.000233589, 0.00311425 and 0.000116794 respectively which implies that DABPRT is better in terms of error than IBP and DART.

It is also evident in Table 4.3 where the MSE of IBP, DART and DABPRT are 0.0000420886, 0.00345648 and 0.0000210443 respectively, so also Table 4.4 with MSE of IBP, DART and DABPRT as 0.00155289, 0.00843556 and 0.000776445 respectively, which makes it evident that the developed DABPRT is better than IBP and DART and gives a better visual quality output than the other techniques.

4.2.3 Structural Similarities (SSIM)

SSIM was also used in the evaluation of the performance of the developed DABPRT reconstruction technique. From Table 4.1, SSIM for MSE for IBP, DART and DABPRT is 1. In

tables 4.2, 4.3 and 4.4, SSIM is also presented as 1; this is because the same level of noise was introduced in the SRR techniques used and the noise in the images reconstructed were totally removed in the process of reconstruction..

4.2.4 Summary of results obtained from the implementation of the developed DABPRT technique

The average of the evaluation results of SRR methods obtained from the images presented in Table 4.5. IBP produced an average PSNR of 82.425dB followed by DART which produced an average of 71.7025dB while the developed DABPRT produced an average PSNR of 85.435dB. IBP produced an average MSE of 0.00077 followed by DART whose average is 0.00479 and the developed DABPRT produced an average MSE of 0.000385 but it was noticed that the Structural Similarity of the three (3) techniques are the same which is 1, this is as a result of significant reduced noise distortion.

It is evident that IBP performs better than DART because the reconstruction error of IBP is lesser than that of DART and this imposed the need for the developed DABPRT approach that combines high performance of IBP with the DART. From the results, it is evident that the developed DABPRT performed better than IBP and DART in PSNR and the error gotten is significantly low than that of IBP and DART which implies that DABPRT produces a better visual quality output than the other techniques.

Figure 4.2 and 4.3 is a bar chart showing the Peak Signal to Noise Ratio (PSNR) and Mean Square Error (MSE) of IBP, DART and the developed DABPRT using the average performance evaluation. Table 4.6 shows the Analysis of variance (ANOVA) test carried out on DART, IBP and the developed DABPRT. The result shows that $F = 367.1454$ and $F_{crit} = 7.708647$. Since

$F > F_{crit}$, where F is Fisher's transformation. Therefore, there is a significant difference between DABPRT over DART and IBP at significance level (α) of 0.05.

4.3 Comparison of the Developed DABPRT Technique with Existing Techniques

The result of the developed technique was evaluated with the results of IBP and DART reconstruction techniques. It can be deduced from Table 4.5 that the developed DABPRT out-performs IBP and DART super resolution reconstruction techniques. This shows that the developed DABPRT produces a high visual quality output than the original IBP and DART super resolution techniques.

The results of the developed technique were compared with existing combination of IBP and DART in Table 4.6. Monalisa (2013) used a combination of IBP and Cuckoo Optimization Algorithm (COA) with levy flights. The results were represented using PSNR, SSIM and MSE. It gives a PSNR of 28.903, SSIM of 0.9999 and MSE of 0.00515. Patel (2013) used IBP combined with edge preserving Infinite Symmetrical Exponential Filter (ISEF) for the reconstruction of low resolution images. The result was presented using PSNR, SSIM and MSE. It gives a PSNR of 33.89, SSIM of 0.9250 and MSE of 0.17765.

Lin (2014) used IBP and edge dominant interpolation for reconstructing low resolution images. It gave a PSNR of 28.743, SSIM of 0.9156 and MSE of 0.20944. Zefreh (2013) also used DART in reconstructing license plates. It gave an average PSNR of 81.229, SSIM of 0.9989 and MSE of 0.007. Figures 4.4(a), 4.4(b) and 4.5 shows a bar chat of PSNR, SSIM and MSE of the developed DABPRT and existing techniques.

From the comparison of existing work and the developed DABPRT, it shows that the developed technique performed better than the compared techniques in terms of PSNR, SSIM and MSE.

Table 4.5 Average of Performance Evaluation Results of the SRR Techniques

SRR Techniques	PSNR	SSIM	MSE
IBP	82.425	1	0.00077
DART	71.7025	1	0.00479
Developed DABPRT	85.435	1	0.000385

Table 4.6 ANOVA for the Average Performance Evaluation of the SRR Techniques

Source of Variation	*SS*	*df*	*MS*	*F*	*P-value*	*F crit*
Between Groups	9564.557174	1	9564.557	367.1454	4.3715E-05	7.708647

Within Groups	104.2045661	4	26.05114
Total	9668.76174	5	

Table 4.7 Comparison of the Developed Technique with Existing Super Resolution Techniques

Authors	SRR Techniques	PSNR	SSIM	MSE

Monalisa (2013)	IBP+COA	28.903	0.9999	0.00515
Patel (2013)	IBP+ISEF	33.89	0.9250	0.17765
Lin (2014)	IBP+edge dominant interpolation	28.743	0.9156	0.20944
Zefreh (2013)	Improved DART	81.229	0.9989	0.007
Olowoye(2016)	Developed DABPRT	85.435	1	0.000385

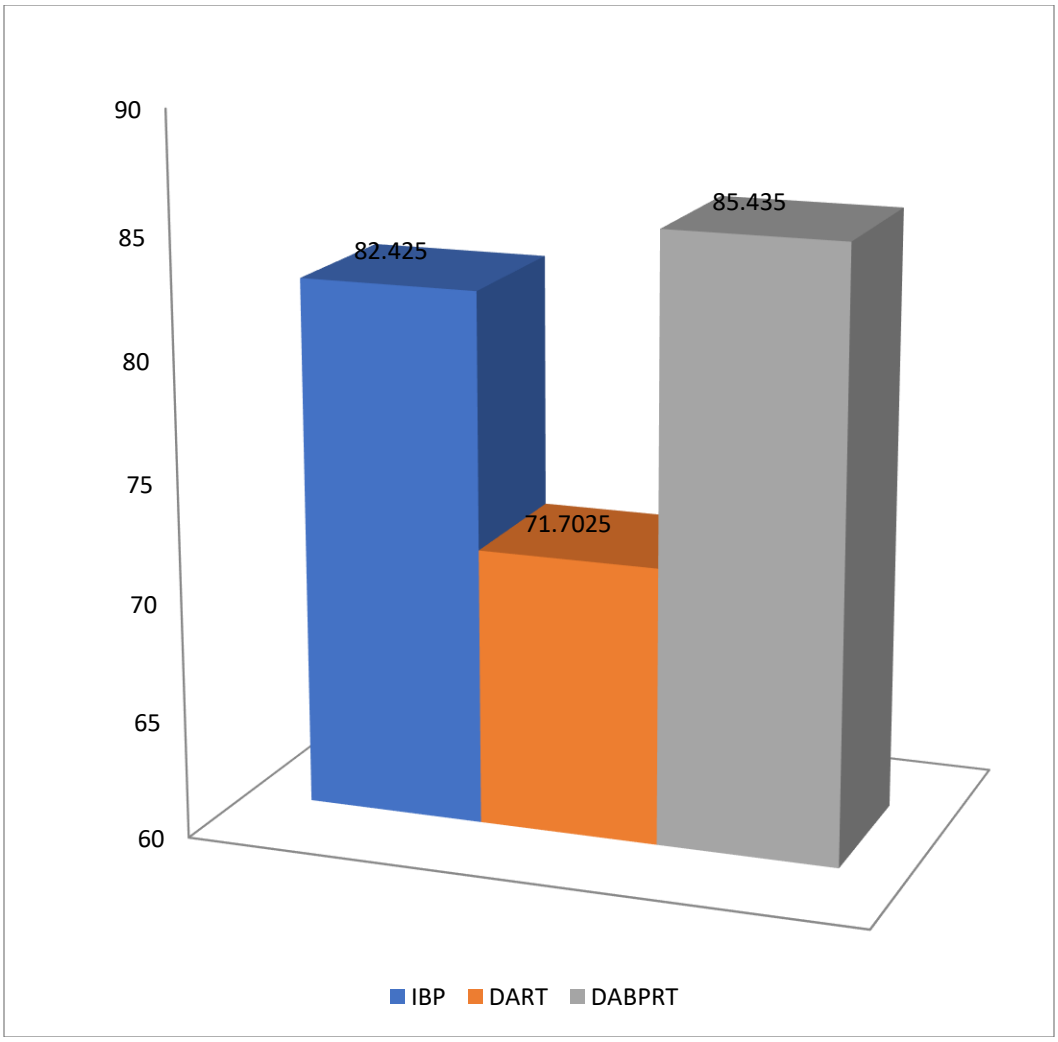

Figure 4.2: Bar Chart showing the average Peak Signal to Noise Ratio of IBP, DART and DABPRT.

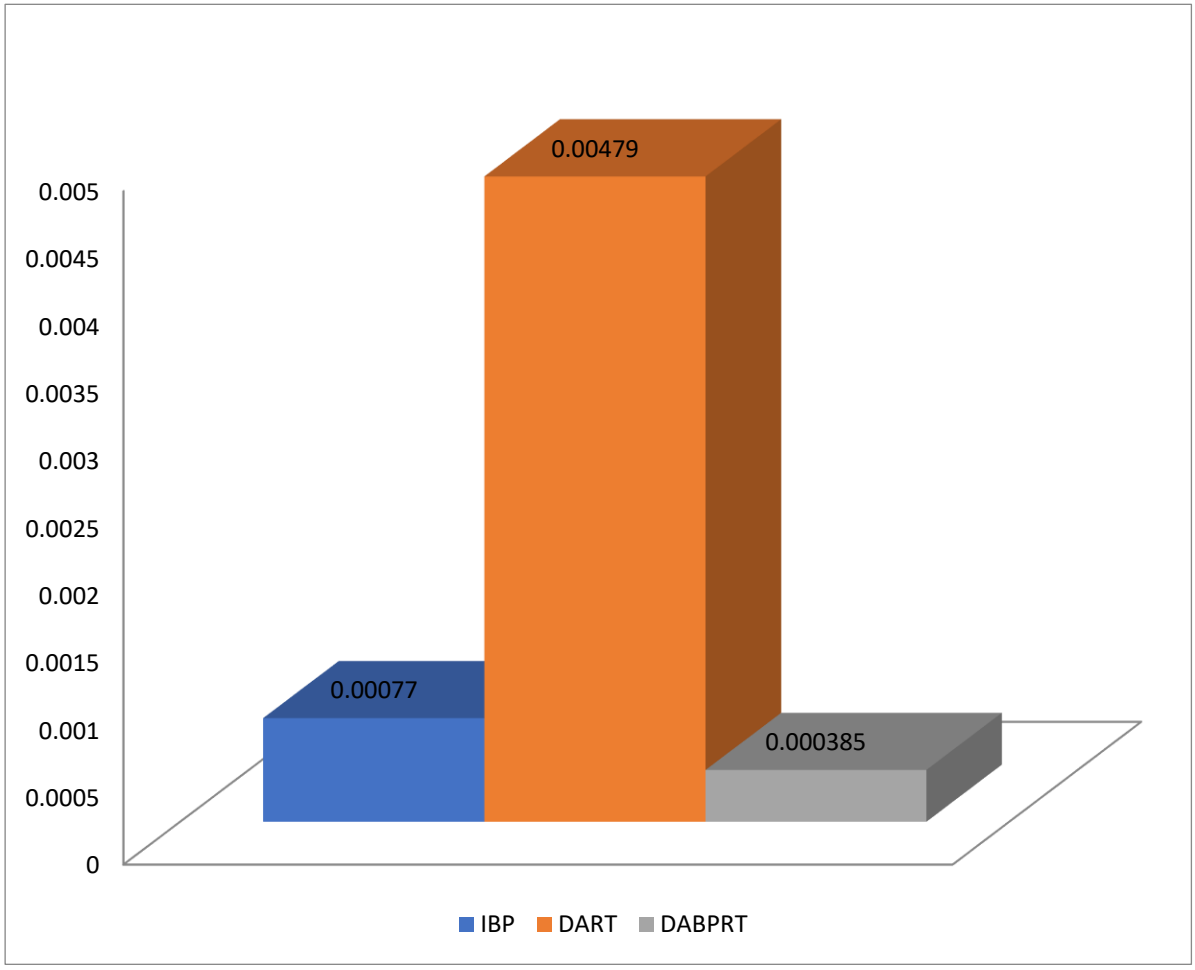

Figure 4.3: Bar Chart showing the average Mean Square Error of IBP, DART and DABPRT.

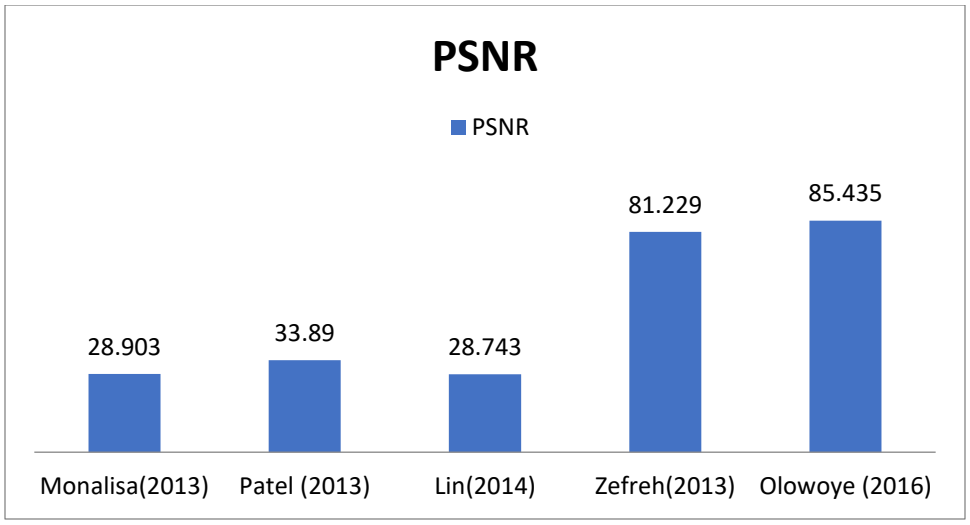

Figure 4.4(a): Bar Chart Showing the PSNR of the Developed Technique and Existing SRR Techniques

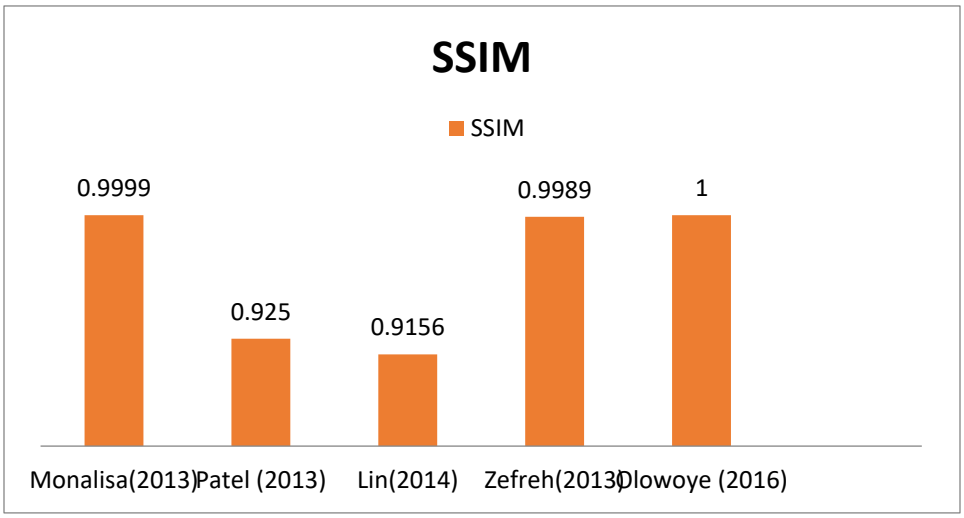

Figure 4.4(b): Bar Chart Showing the SSIM of the Developed Technique and Existing SRR Techniques

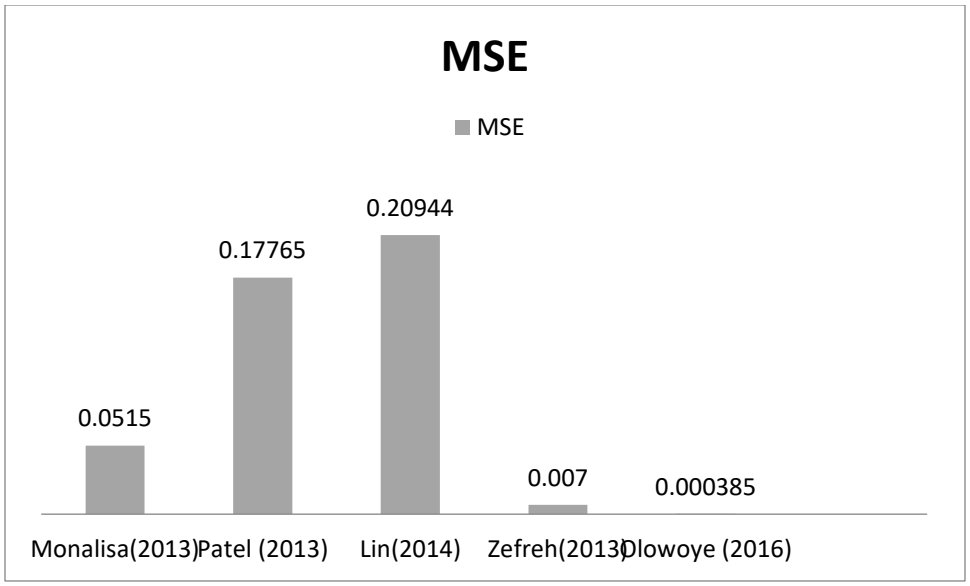

Figure 4.5: Bar Chart Showing the MSE of the Developed Technique with Existing SRR Techniques

CHAPTER FIVE

CONCLUSION AND RECOMMENDATION

5.1 Conclusion

A Discrete Algebraic Back Projection Reconstruction Technique (DABPRT) was developed to solve the low resolution challenge associated with images captured using low resolution mobile capturing devices. The developed technique is composed of a combination of Discrete Algebraic Reconstruction Technique (DART) and Iterative Back Projection (IBP). The performance of the developed DABPRT was evaluated using Peak Signal to Noise Ratio (PSNR), Structural Similarity (SSIM) and Mean Square Error (MSE).

The developed technique produced the highest average PSNR value of 85.425dB and SSIM of 1 which implies that the images reconstructed by this have improved visual quality and reduced noise than those produced by DART and IBP. DABPRT also provided the lowest average MSE of 0.000385 which implies that the error produced by the developed technique is significantly lower than that provided by DART and IBP.

Conclusively, the developed DABPRT has not only led to an improved PSNR and significantly reduced MSE but it also provides a significant outcome in the reconstruction of low resolution images obtained from low resolution mobile capturing devices with improved output. The developed technique can be applied to various field of life including medicine, security and surveillance systems among others.

5.2 Contribution to Knowledge

This research work has contributed the following to knowledge:

i. Development of a combination of DART and IBP for the reconstruction of low resolution images with reduced reconstruction error.

ii. Production of a better visual quality output image with reduced noise and preserved edge information.

5.3 Recommendations

Future work can focus on the application of the developed DABPRT technique to video frames and be incorporated to extract features from images. Also, computational time can be applied as an evaluation metrics for the technique.

REFERENCES

Agrawal, M. (2013). Development of image super resolution algorithm. Thesis for the degree of Master of Technology, Department of Computer Science and Engineering, National Institute of Technology, Rourkela, India, 31-50.

Amit, T. and Avinash, D. (2013). Object recognition from image using Grid Base Color Moment feature extraction method.*International Journal of research in engineering and technology*, 2(3): 333-336.

Anil, B. G. and Vijay, S. R. (2014). A survey on image reconstruction using super resolution, 1-8.

Ansari, I. A. and Borse, R. Y. (2013). Image processing and Analysis.*International Journal of Engineering Research and Applications*, 3(4): 1655-1658.

Badano, A. (2015). Consistence and standardization of color in Medical Imaging: a consensus report.*Journal of Digital Imaging*, 28(1): 41-52.

Baker, S. and Kanade, T. (2002). Limits on super-resolution and how to break them.*IEEE Transactions on Pattern Analysis and Machine Intelligence*, 24(9): 1167-1183.

Batenburg, K. J., Sijbers J.,Poulsen H. F. and Knudsen E. B. (2010). DART: a robust algorithm for fast reconstruction of three-dimensional grain maps. *Journal of Applied Crystallography*, 43(6): 1464–1473.

Bengtsson, T. (2013). Towards Joint Super-Resolution and High Dynamic Range Image Reconstruction. *A Thesis submitted for the degree of Licentiate of Engineering to the Department of Signals and Systems, Chalmers University of Technology, Goteborg, Sweden*, 12-25.

Bernard, G. and Gernot, K. (2013). Information Loss and Anti-Aliasing Filters in Multirate System.*IEEE Forum on Signal Processing for RF-Systems*, 1-12.

Capel, D. and Zisserman, A. (2003). Computer vision applied to super resolution.*IEEE Signal Processing Magazine*, 20(3): 75-86.

Chang, H., Yeung, D. Y., and Xiong, Y. (2004). Super-resolution through neighbor embedding.*Proceedings of IEEE Computer Society Conference on Computer Vision and Pattern Recognition*, 1: 275-282.

Chung, J., Haber, E., and Nagy, J. (2006). Numerical methods for coupled super resolution. *Inverse Problems*, 22(4): 1261-1272.

Datsenko, D. andElad, M. (2007). Example-based single document image super resolution: a global MAP approach with outlier rejection. *Multidimensional System and Signal Processing*, 18(2-3):103-121.

Elad, M. and Feuer, A. (1997). Restoration of single super-resolution image from several blurred, noisy and down-sampled measured images. *IEEE Transaction on Image Processing*, 6(12):1646-1658.

Elad, M.,Farsiu, S., Robinson, D. and Milanfar, P. (2004). Advances and challenges in super resolution. *International Journal of Imaging Systems and Technology*, 14(2):47-57.

Fagbola T. M. (2015). A Pose Illumination Invariant Feature Extraction Technique for Low Resolution Video feeds. A thesis submitted to the Department of Computer Science, Faculty of Engineering and Technology, Ladoke Akintola University, Ogbomoso, Oyo State, Nigeria, 50-120.

Fan,Y., Gan,Z., Qiu,Y. and Zhu,X. (2011). Single image super resolution method based on edge preservation. *In Image and Graphics 6th International Conference*, 394-399.

Farsiu, S., Robinson, D., Elad, M., and Milanfar, P. (2004). Fast and robust multi-frame super resolution. *IEEE Transaction on Image Processing*, 13(10):1327-1344.

Farsiu, S. (2004). Advances and challenges in super-resolution. *International Journal of Imaging Systems and Technology*, 14(2): 47-57.

Freeman, W. T., Jones, T. R., and Pasztor, E. C. (2002). Example-based super resolution. *IEEE Computer Graphics and Applications*, 22(2):56-65.

GaidhaniPradeep (2012):"Super resolution", http://homepages.inf.ed.ac.uk/rbf/CVonline/LOCAL_COPIES/AV1011/Super_Resolution_CVonline.pdf

Huang, T. S., Yang, J., Wright, J. and Ma, Y. (2009). Super-resolution via sparse representation. *IEEE Transactions on Image Processing*, 1-9.

Irani, M. and Peleg, S. (1991). Improving resolution by image registration. Graphical *Models and Image Processing*, 5(3): 231-239.

Irani, M. and Peleg, S. (1993). Motion analysis for image enhancement: resolution, occlusion, and transparency. *Journal of Visual Communication and Image Representation*, 4(4):324-335.

Jianchao, Yang, John, Wright, Thomas, Huang, and Yi, Ma (2008). Image super resolution as sparse representation of raw image patches. *In Proceedings of IEEE Computer Society Conference on Computer Vision and Pattern Recognition*, 1-8.

Joyce, E. Farrell and Brian, A. Wandell (2015). Handbook of Digital Imaging. *DOI: 10.1002/9781118798706.hdi013*

Jyoti, Dadwal and Bhubneshwar, Sharma (2015). Design of Image Processing Technique in Digital Enhancement Application. *International Journal of Advances in Scientific Research*, 1(8):340-342.

Kavita, Rikita Saroha, RajaniBala, SunitaSiwach (2013). Overview of Image Processing and Image Segmentation. *International journal of Research in Computer applications and Robotics*. 1(7): 1-13.

Kim, S. P., Bose, N. K., and Valenzuela, H. M. (1990). Recursive reconstruction of high resolution image from noisy under sampled multiframes. *IEEE Transactions on Acoustics, Speech and Signal Processing*, 38(6):1013-1027.

Levin, A., Weiss, Y., Durand, F., and Freeman, W. (2009). Understanding and evaluating blind deconvolution algorithms. *In Proceedings of IEEE Computer Society Conference on Computer Vision and Pattern Recognition*, 1964-1971.

Lin, G. and Lai, M. (2008). Enhancing resolution using iterative back-projection technique for image sequences. *Journal of Computers*, 19(3): 44-54.

Lin, Chi-Kun, Yi-Hsien, Wu, Jar-Ferr, Yang, and Bin-Da, Liu (2014). An Iterative Back Projection Super Resolution Algorithm for Low Resolution Image Up-sampling, 1-5.

Marcia, L., Aguena, S., Nelson, D., Mascarenha, A. (2011). Generalization of Iterative Restoration Techniques for Super-Resolution. *UFSCar - Universidade Federal de Sao Carlos Sao Carlos, SP – Brazil*, 32-50.

Merugu, Suresh, Kamal, Jain (2013). Colorimetrically resolution enhancement method for satellite imagery to improve land use. *14thEsri India User Conference*, 7-15.

Milanfar, Peyman(2010). Super resolution: imaging. *Published by CRC press*, 3-10.

Monalisa, R. (2013). Spatial super resolution based image reconstruction using IBP and Evolutionary method. *An M.tech thesis submitted to Department of Electrical Engineering, National Institute of Technology Rourkela, Odisha, India*, 20-30.

Muzamil, Bhat (2014). Digital Image Processing. *International Journal of Scientific and Technology Research*, 3(1):272-276.

Nguyen, N., Milanfar, P., and Golub, G. H. (2001). A computationally efficient image super resolution algorithm. *IEEE Transactions on Image Processing*, 10(5):573-583.

Oppenheium, A. V. and Schafer, R.W. (2010). Discrete-Time Signal Processing. *3rd ed. Upper Saddle River. NJ: Pearson Higher Ed*, 25-40.

Park, Sung C., Park, Min K., and Kang, Moon G. (2003). Super-resolution image reconstruction: a technical overview. *IEEE Signal Processing Magazine*,20(3):21-36.

Patel, Shreyas A. (2013). Novel Iterative Back Projection Approach. *IOSR Journal of Computer Engineering (IOSR-JCE)*, 11(1): 65-69.

Patti, A. J., Sezan, M. I, and Tekalp, A. M. (1997). Robust methods for high quality stills from interlaced video in the presence of dominant motion. *IEEE Transactions on Circuits and Systems for Video Technology*, 7(2):328-342.

Patti, A. J., Sezan, M. I., and Tekalp, A. M. (1997). Super resolution video reconstruction with arbitrary sampling lattices and nonzero aperture time. *IEEE Transactions on Image Processing*, 6(8): 1064-1076.

Pickup, L. C., Capel, D. P., Roberts, S. J., and Zisserman, A. (2009). Bayesian methods for image super-resolution. *The Computer Journal*, 52(1):101-113.

Pickup, L. C., Robert, S. J., and Zisserman, A. (2003). A sampled texture prior for image super resolution. *In Proceedings of Advances in Neural Information and Processing System*, 1587-1594.

Proakis, John (2000). Digital Signal Processing: Principles, Algorithms and Applications. *(3rd ed.). India: Prentice-Hall. ISBN: 8120311299*, 20-25.

Protter, M., Elad, M., Takeda, H., and Milanfar, P. (2009). Generalizing the nonlocal-means to super resolution reconstruction. *IEEE Transactions on Image Processing*, 18(1):36-51.

Ramesh K. (2012). Digital Photoelasticity: Advance Techniques and Applications. *Springer Science & Business Media*, 67-75.

Rao, Ch.Venkateswara, Srinivasa, Rao V., Srinivas, K., Hima, Deepthi V. and Kusuma, Kumari E. (2013). Robust high resolution image from the low resolution satellite image. *International conference on advances in computer science*, *AETAC* 4(56): 26-36

Rao, K.M.M (2006). Overview of Image Processing. *Readings in Image Processing*, 1-7.

Robinson, D. and Milanfar, P. (2004). Fundamental performance limits in image registration. *IEEE Transactions on Image Processing*, 13(9):1185-1199.

Rudin, L., Osher, S., and Fatemi, E. (1992). Nonlinear total variation based noise removal algorithms. *Physica D: Nonlinear Phenomena*, 60(1-4):259-268.

Rujul, R Makwana, Nita, D Mehta (2013). Single image super resolution VIA iterative back projection based canny edge detection and a gabor filter prior. *International Journal of Soft Computing and Engineering (IJSCE)*, 3(1): 379-384.

Schultz, R. R. and Stevenson, R. L. (1994). A Bayesian approach to image expansion for improved definition. *IEEE Transactions on Image Processing*, 3(3): 233-242.

Schultz, R. R. and Stevenson, R. L. (1996). Extraction of high resolution frames from video sequences. *IEEE Transactions on Image Processing*,5(6): 996-1011.

Segall, C. A., Katsaggelos, A. K., Molina, R., and Mateos, J. (2004). Bayesian resolution enhancement of compressed video. *IEEE Transactions on Image Processing*, 13(7):898-910.

Shashi, Rathore, Harshalatha, Y. (2012). Iterative Back-Projection Algorithm Based Signal Processing Approach To Enhance An Image Resolution. *International Journal of Engineering Research and Applications (IJERA)*, 2(6):1449-1454.

Shen, H., Zhang, L., Huang, B., and Li, P. (2007). A MAP approach for joint motion estimation, segmentation and super-resolution. *IEEE Transactions on Image Processing*, 16(2):479-490.

Siddique, Muhammad (2012). Performance Evaluation of Super -Resolution Reconstruction Algorithms Based On Linear Magnifications. 20-35.

Sonali, Shejwal, Deshpande, A. M. (2014). Comparative analysis of edge based single image super resolution. *In International Journal of Computer Trends and Technology (IJCTT)*, 10(5): 257-261.

Stark, H. and Oskoui, P. (1989). High-resolution image recovery from image plane arrays, using convex projections. *Journal of Optical Society of America A*, 6(11):1715-1726.

Su, W. and Kim, S. P. (1994). High-resolution restoration of dynamic image sequences. *International Journal of Imaging Systems and Technology*,5(4):330-339.

Sun, J., Zheng, N. N., Tao, H.and Shum, H.(2003). Image hallucination with primal sketch priors. *In Proceedings of IEEE Computer Society Conference on Computer Vision and Pattern Recognition*, 2: 729-736.

Tikhonov, A. N. and Arsenin, V. A. (1997). Solution of ill-posed problems. *Winston & Sons, Washington*, 20-28.

Tipping, Michael E. and Bishop, Christopher M. (2003). Bayesian image super resolution. *In Proceedings of Advances in Neural Information Proceeding Systems*, 1279-1286.

Tom, B. C. and Katsaggelos, A. K. (1995). Reconstruction of a high-resolution image by simultaneous registration, restoration and interpolation of low resolution images. *In Proceedings of the IEEE International Conference on Image Processing*, 2(1): 2539-2545.

Tom, B. C., Katsaggelos, A. K., and Galatsanos, N. P. (1994). Reconstruction of a high resolution image from registration and restoration of low resolution images. *In Proceedings of IEEE International Conference on Image Processing*: 553-557.

Tsai, R. Y. and Huang, T. S. (1984). Multiple frame image restoration and registration. *In Advances Computer Vision and Image Processing, Greenwich, CT: JAI Press Inc.*, 317-339.

Van, Gompel G., Batenburg, K.J., Van, de Casteela E., Van, Aarle W., Sijbers, J (2010). A discrete tomography approach for super resolution micro-CT images: application to bone. *Biomedical Imaging: From Nano to Macro, Rotterdam*, 816-819.

Villena, S., Vega, M., Babacan, S. D., Molina, R. and Katsaggelos, A. K. (2012). Bayesian Combination of Sparse and Non-Sparse Priors in Image Super Resolution. *IEEE International Conference on Image Processing*, 1-24.

Wang, Jong-Tzy, Liang, Kai-Wen, Chang, Shu-Fan, and Chang, Pao-Chi (2009). Super Resolution Image with Estimated High Frequency Compensated Algorithm. *ISCIT*, 6(9): 175-180.

Wang, Q., Tang, X., and Shum, H. (2005). Patch based blind image super resolution. *In Proceedings of IEEE International Conference on Computer Vision*, 1:709-716.

Wang, and Yanfei (2011). Optimization and regularization for computational inverse problems and applications. Springer.

Weisheng, Dong, Lei, Zhang, Guangming, Shi and Xiaolin, Wu (2009). Non-local Back Projection for Adaptive Image Enlargement. *In proceedings of the international conference on image processing, ICIP, Cairo, Egypt*.

Wim van Aarle, Kees Joost Batenburg, Gert Van Gompel, Elke Van de Casteele, and Jan Sijbers (2014). Super-Resolution for Computed Tomography Based on Discrete Tomography. In IEEE Transactions On Image Processing, 23(3): 1181-1193.

Woods, N. A., Galatsanos, N. P., and Katsaggelos, A. K. (2006). Stochastic methods for joint registration, restoration and interpolation of multiple under sampled images. *IEEE Transactions on Image Processing*,15(1):210-213.

Yedidia, J. S., Freeman, W. T., and Weiss, Y. (2001). Generalized belief propagation. *In Proceedings of Advances in Neural Information Processing Systems*, 689-695.

Yixiong, Zhang, Mingliang, Tao, Kewei, Yang, and Zhenmiao, Deng (2015). Video Super-resolution Reconstruction Using Iterative Back Projection with Critical-Point Filters Based Image Matching. *Advances in Multimedia*, 1-10.

Youla, D. C. and Webb, H. (1982). Image registration by the method of convex projections: Part 1-thoery. *IEEE Transactions on Medical Imaging*, 1(2):81-94.

Zefreh, Karim Zarei, AarleWim, van, Batenburg, K. Joost and Sijbers, Jan (2013). Discrete Algebraic Reconstruction Technique: A New Approach for Super Resolution Reconstruction of License Plates. *Journal of Electronic Imaging* 22(4): 041111-1-041111-7.

APPENDIX A

SOURCE CODES FOR EXISTING TECHNIQUES

CODE FOR IBP

```
% Adapted from: Victor May: mayvic(at)gmail(dot)com

% A simple implementation of a gradient descent optimization.

function x = ibp(lhs, rhs, initialGuess, iteration)
   maxIter = iteration;
   iter = 0;
   eps = 0.01;

   x = initialGuess;
   res = lhs' * (rhs - lhs * x);
   mse = res' * res;
   mse0 = mse;
   while (iter < maxIter && mse > eps^2 * mse0)
       res = lhs' * (rhs - lhs * x);
       x = x + res;
       mse = res' * res;
       fprintf(1, 'Gradient Descent Iteration %d mean-square error %3.3f\n', iter,
mse);
       iter = iter + 1;
   end

end
```

CODE FOR DART

```
function [X,info] = dart(A,b,K,x0,options)
%KACZMARZ Kaczmarz's method (often referred to as ART)
%
%   [X,info] = kaczmarz(A,b,K)
%
% Implements Kaczmarz's method for the system Ax = b:
%
%       x^{k+1} = x^k + lambda*(b_i - a^i'*x^k)/(||a^i||_2^2)*a^i
%
% where a_i' is the i-th row of A, and i = (k mod m) + 1.
%
% Input:
%   A        m times n matrix.
%   b        m times 1 vector.
%   k        Number of iterations. If K is a scalar, then K is the maximum
%            number of iterations and only the last iterate is saved.

% Maria Saxild-Hansen and Per Chr. Hansen, July 5, 2015, DTU Compute.

% Reference: G. T. Herman, Fundamentals of Computerized Tomography,
% Image Reconstruction from Projections, Springer, New York, 2009.

[m,n] = size(A);
A = A';  % Faster to perform sparse column operations.

% Check the number of inputs.
if nargin < 3
    error('Too few input arguments')
end
```

```
% Default value of starting vector x0.
if nargin < 4 || isempty(x0)
    x0 = zeros(n,1);
end

% The sizes of A, b and x must match.
if size(b,1) ~= m || size(b,2) ~= 1
    error('The sizes of A and b do not match')
elseif size(x0,1) ~= n || size(x0,2) ~= 1
    error('The size of x0 does not match the problem')
end

% Initialization.
if nargin < 5
    if isempty(K)
        error('No stopping rule specified')
    end
    stoprule = 'NO';
    lambda = 1;
    Knew = sort(K);
    kmax = Knew(end);
    X = zeros(n,length(K));

    % Default is no nonnegativity or box constraint or damping.
    nonneg = false;
    boxcon = false;
    damp = 0;

else
% Check the contents of options, if present.

    % Nonnegativity.
    if isfield(options,'nonneg')
        nonneg = options.nonneg;
    else
        nonneg = false;
    end

    % Box constraints [0,L].
    if isfield(options,'box')
        nonneg = true;
        boxcon = true;
        L = options.box;
    else
        boxcon = false;
    end

    % Damping.
```

APPENDIX B

CODES FOR THE DEVELOPED DABPRT

CODES FOR CREATING LOW RESOLUTION IMAGES

```
% Tests

function [ images croppedOriginal] = CreateLowResImgs(X, Inputx)
```

```
%% load image

numImages = Inputx.numImages; % number of LR images to create

tx = Inputx.tx; %translation parameter x maximum 50 step 5
ty = Inputx.ty; %translation parameter y maximum 50 step 5
theta = Inputx.theta; % the rotation angle maximum 45 step 5

blurSigma = Inputx.blurSigma; % standard deviation
df = Inputx.tf; % downsampling factor
V = Inputx.V; % noise variance

    padRatio = 0.2;

    workingRowSub = round(0.5 * padRatio * size(X, 1)) : round((1 - 0.5 * padRatio) *
size(X, 1));
    workingColSub = round(0.5 * padRatio * size(X, 2)) : round((1 - 0.5 * padRatio) *
size(X, 2));

    croppedOriginal = X(workingRowSub, workingColSub);

    X = croppedOriginal;
[rw,cl] = size(X);

    for i = 1 : numImages

        %% Test geometric warping (translation & rotation)


        %==== translation
        Xt = translate(X,tx(i),ty(i));

        %==== rotation
        W = rotation(Xt,theta(i));

        %=====
        x = size(W,1)-(rw-1); y=size(W,2)-(cl-1);

        W_im = W(x:end,y:end);

        %%  blurring (sensor averaging)

        Bl_im = imgaussfilt(W_im, blurSigma);

        %% downsampling (undersampling & aliasing)

        Dn_im = Bl_im(1:df:end,1:df:end);

        %% additive noise

        Ns_im = imnoise(Dn_im,'gaussian',0,V); %  observed LR image

        images{i} = Ns_im;
    end
```

```
end
```

CODE FOR DABPRT

```
% Discrete Algebraic Back Projection Technique (DABPT)
% for the reconstruction of low resolution images

close all; clear; clc;

%% convert high resolution (HR) image to low resolution (LR) images

N = 2; % number of LR images to generate - observed images

%========== input HR image

pth = cd;
[FileName,PathName]= uigetfile('*.bmp;*.BMP;*.tif;*.TIFF;*.jpg;*.JPEG','Input an RGB
image');
if FileName ~= 0
    cd(PathName);

    imfile=strcat(PathName,num2str(FileName));

    Im_rgb=imread(imfile); % reference image

    if ndims(Im_rgb) == 3; X = rgb2gray(Im_rgb); end  % Color Images
end
cd(pth);


imshow(X),title('original image')

%========== geometric warping (translation & rotation)


%========== blurring (sensor averaging)


%========== down-sampling (undersampling & aliasing)


%========== noise (sensor noise)
```

CODE FOR DABPRT GUI

```
function varargout = GUI_DABPRT(varargin)
% GUI_DABPRT MATLAB code for GUI_DABPRT.fig
%      GUI_DABPRT, by itself, creates a new GUI_DABPRT or raises the existing
%      singleton*.
%
%      H = GUI_DABPRT returns the handle to a new GUI_DABPRT or the handle to
%      the existing singleton*.
%
%      GUI_DABPRT('CALLBACK',hObject,eventData,handles,...) calls the local
%      function named CALLBACK in GUI_DABPRT.M with the given input arguments.
%
%      GUI_DABPRT('Property','Value',...) creates a new GUI_DABPRT or raises the
```

```
%      existing singleton*.  Starting from the left, property value pairs are
%      applied to the GUI before GUI_DABPRT_OpeningFcn gets called.  An
%      unrecognized property name or invalid value makes property application
%      stop.  All inputs are passed to GUI_DABPRT_OpeningFcn via varargin.
%
%      *See GUI Options on GUIDE's Tools menu.  Choose "GUI allows only one
%      instance to run (singleton)".
%
% See also: GUIDE, GUIDATA, GUIHANDLES

% Edit the above text to modify the response to help GUI_DABPRT

% Last Modified by GUIDE v2.5 14-May-2016 21:29:14

% Begin initialization code - DO NOT EDIT
gui_Singleton = 1;
gui_State = struct('gui_Name',       mfilename, ...
                   'gui_Singleton',  gui_Singleton, ...
                   'gui_OpeningFcn', @GUI_DABPRT_OpeningFcn, ...
                   'gui_OutputFcn',  @GUI_DABPRT_OutputFcn, ...
                   'gui_LayoutFcn',  [] , ...
                   'gui_Callback',   []);
if nargin && ischar(varargin{1})
    gui_State.gui_Callback = str2func(varargin{1});
end

if nargout
    [varargout{1:nargout}] = gui_mainfcn(gui_State, varargin{:});
else
    gui_mainfcn(gui_State, varargin{:});
end
% End initialization code - DO NOT EDIT
clear; clc;


% --- Executes just before GUI_DABPRT is made visible.
function GUI_DABPRT_OpeningFcn(hObject, eventdata, handles, varargin)
% This function has no output args, see OutputFcn.
% hObject    handle to figure
% eventdata  reserved - to be defined in a future version of MATLAB
% handles    structure with handles and user data (see GUIDATA)
% varargin   command line arguments to GUI_DABPRT (see VARARGIN)

% Choose default command line output for GUI_DABPRT
handles.output = hObject;

% Update handles structure
guidata(hObject, handles);

% UIWAIT makes GUI_DABPRT wait for user response (see UIRESUME)
% uiwait(handles.GUI_DABPRT);


sld_iterationHndl = findobj('Tag','sld_iteration');
sld_xy_dispHndl = findobj('Tag','sld_xy_disp');
```

```
sld_angleHndl = findobj('Tag','sld_angle');
sld_noiseHndl = findobj('Tag','sld_noise');
sld_blurHndl = findobj('Tag','sld_blur');
sld_img_numHndl = findobj('Tag','sld_img_num');

txt_iterationHndl = findobj('Tag','txt_iteration');
txt_xy_dispHndl = findobj('Tag','txt_xy_disp');
txt_angleHndl = findobj('Tag','txt_angle');
txt_noiseHndl = findobj('Tag','txt_noise');
txt_blurHndl = findobj('Tag','txt_blur');
txt_img_numHndl = findobj('Tag','txt_img_num');

set(txt_iterationHndl,'String', num2str(get(sld_iterationHndl,'value')));
set(txt_xy_dispHndl,'String', num2str(get(sld_xy_dispHndl,'value')));
set(txt_angleHndl,'String', num2str(get(sld_angleHndl,'value')));
set(txt_noiseHndl,'String', num2str(get(sld_noiseHndl,'value')));
set(txt_blurHndl,'String', num2str(get(sld_blurHndl,'value')));
set(txt_img_numHndl,'String', num2str(get(sld_img_numHndl,'value')));

btnCreateLRimgsHndl = findobj('Tag','btnCreateLRimgs');
set(btnCreateLRimgsHndl,'Enable','off');
btnIBPHndl = findobj('Tag','btnIBP');
set(btnIBPHndl,'Enable','off');
btnDARTHndl = findobj('Tag','btnDART');
set(btnDARTHndl ,'Enable','off');
btnDABPRTHndl = findobj('Tag','btnDABPRT');
set(btnDABPRTHndl,'Enable','off')

%mp=cd; mp=char(mp);setappdata(handles.GUI_DABPRT,'rootdir',mp);


% --- Outputs from this function are returned to the command line.
function varargout = GUI_DABPRT_OutputFcn(hObject, eventdata, handles)
% varargout  cell array for returning output args (see VARARGOUT);
% hObject    handle to figure
% eventdata  reserved - to be defined in a future version of MATLAB
% handles    structure with handles and user data (see GUIDATA)

% Get default command line output from handles structure
varargout{1} = handles.output;


% --- Executes on button press in btnRefImage.
function btnRefImage_Callback(hObject, eventdata, handles)
% hObject    handle to btnRefImage (see GCBO)
% eventdata  reserved - to be defined in a future version of MATLAB
% handles    structure with handles and user data (see GUIDATA)
global imfile
global FileName

pth = cd;
[FileName,PathName]= uigetfile('*.bmp;*.BMP;*.tif;*.TIF;*.jpg','Open an image');
if FileName ~= 0
    cd(PathName);
```

```
    imfile=strcat(PathName,num2str(FileName));
    %Image_original(imfile);
    Im=imread(imfile);
    Im=imresize(Im,[128 128]);
    %Im=rgb2gray(Im);
    if ndims(Im) == 3;
       Im = im2double(rgb2gray(Im));
    end  % Color Images

    axes(findobj('Tag','axes1'))
    %imshow(FileName),title('original image')
    imshow(Im),title('Reference image')

    setappdata(findobj('Tag','GUI_DABPRT'),'refImg',Im);

    btnCreateLRimgsHndl = findobj('Tag','btnCreateLRimgs');
    set(btnCreateLRimgsHndl,'Enable','on');

end
cd(pth);
```

APPENDIX C

GUIs

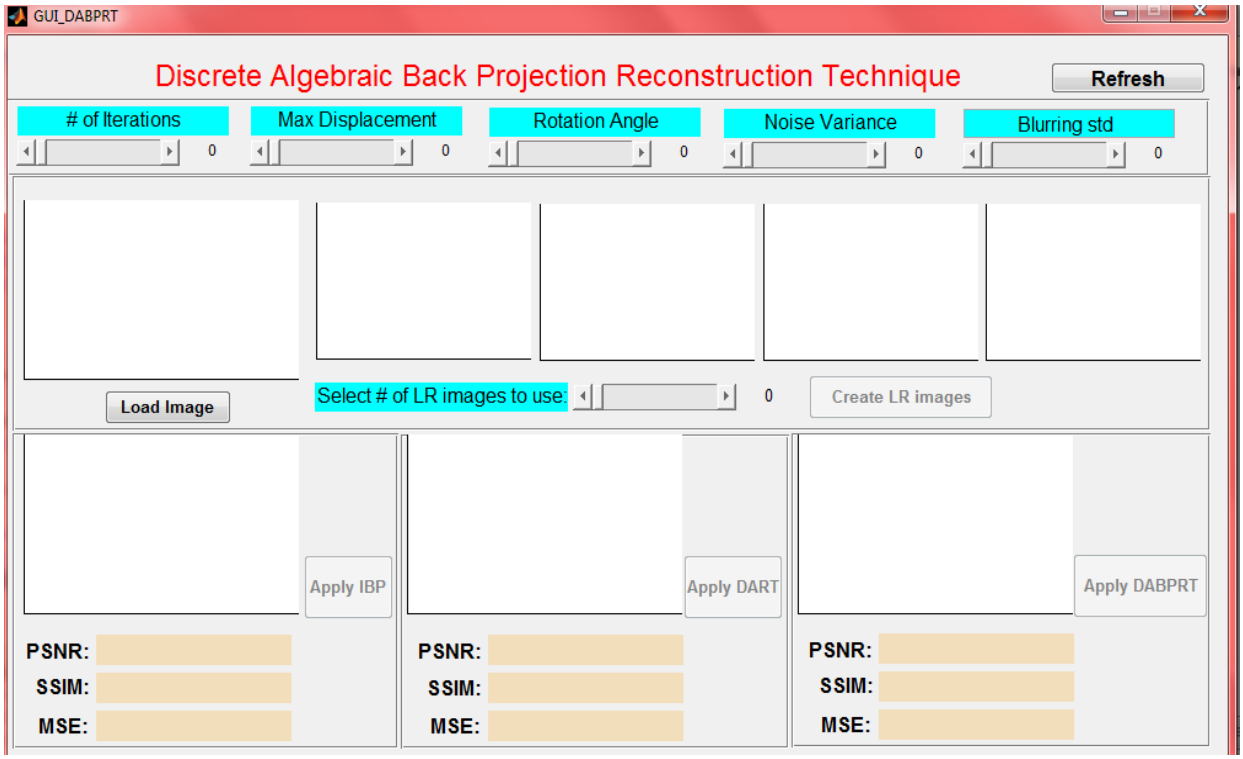
GUI_DABPRT
Discrete Algebraic Back Projection Reconstruction Technique
Refresh
# of Iterations
Max Displacement
Rotation Angle
Noise Variance
Blurring std
0
0
0
0
0
Load Image
Select # of LR images to use:
0
Create LR images
Apply IBP
Apply DART
Apply DABPRT
PSNR:
SSIM:
MSE:
PSNR:
SSIM:
MSE:
PSNR:
SSIM:
MSE:

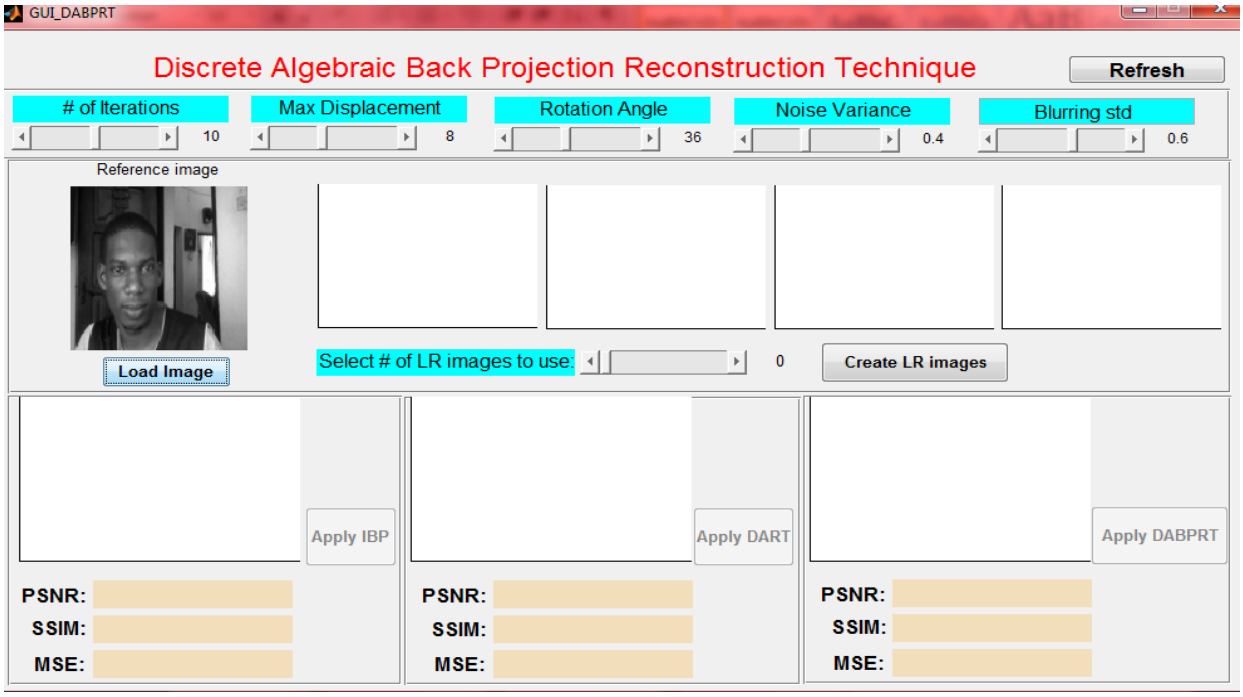
GUI_DABPRT
Discrete Algebraic Back Projection Reconstruction Technique
Refresh
# of Iterations
Max Displacement
Rotation Angle
Noise Variance
Blurring std
10
8
36
0.4
0.6
Reference image
Load Image
Select # of LR images to use:
0
Create LR images
Apply IBP
Apply DART
Apply DABPRT
PSNR:
SSIM:
MSE:
PSNR:
SSIM:
MSE:
PSNR:
SSIM:
MSE:

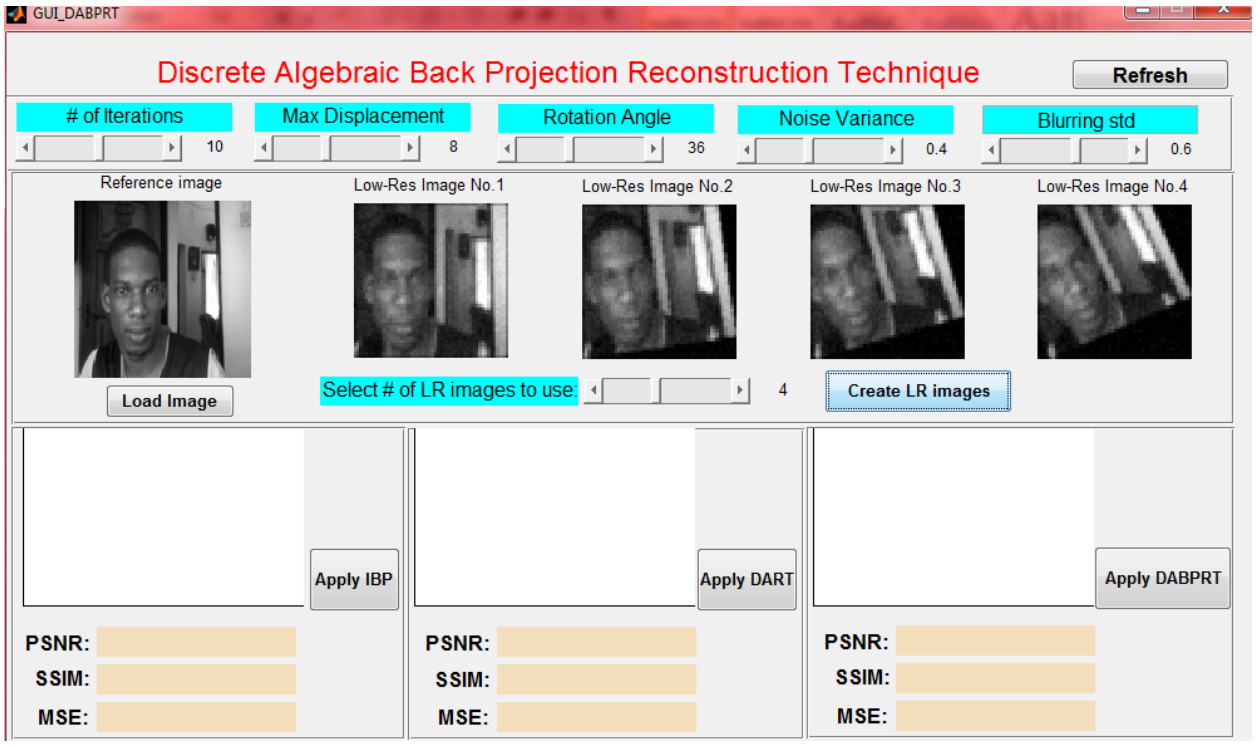
GUI_DABPRT
Discrete Algebraic Back Projection Reconstruction Technique
Refresh
# of Iterations
10
Max Displacement
8
Rotation Angle
36
Noise Variance
0.4
Blurring std
0.6
Reference image
Low-Res Image No.1
Low-Res Image No.2
Low-Res Image No.3
Low-Res Image No.4
Load Image
Select # of LR images to use:
4
Create LR images
Apply IBP
Apply DART
Apply DABPRT
PSNR:
SSIM:
MSE:
PSNR:
SSIM:
MSE:
PSNR:
SSIM:
MSE:

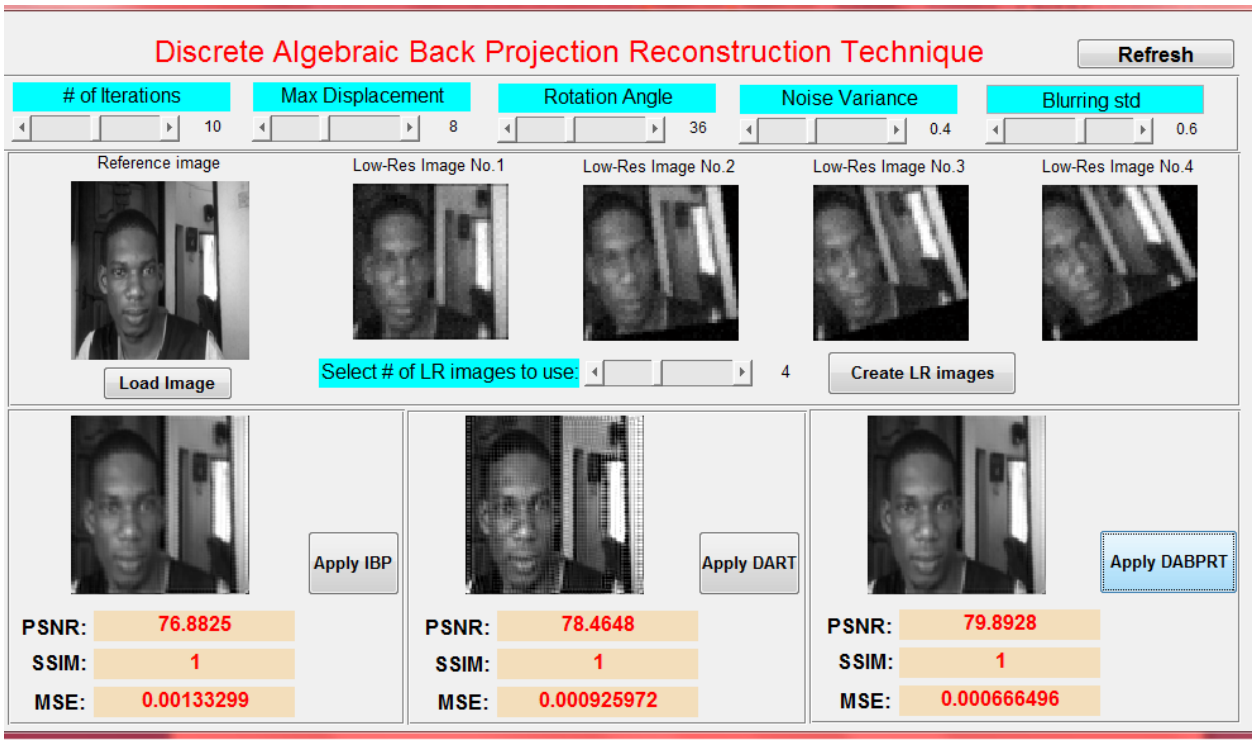
Discrete Algebraic Back Projection Reconstruction Technique
Refresh
# of Iterations
10
Max Displacement
8
Rotation Angle
36
Noise Variance
0.4
Blurring std
0.6
Reference image
Low-Res Image No.1
Low-Res Image No.2
Low-Res Image No.3
Low-Res Image No.4
Load Image
Select # of LR images to use:
4
Create LR images
Apply IBP
Apply DART
Apply DABPRT
PSNR:
76.8825
SSIM:
1
MSE:
0.00133299
PSNR:
78.4648
SSIM:
1
MSE:
0.000925972
PSNR:
79.8928
SSIM:
1
MSE:
0.000666496